JGR Atmospheres

Key Points:
- The grid resolution of atmospheric models has become fine enough that are able to partially resolve turbulent motions in the boundary layer
- This resolution regime comprises the turbulence "gray zone" where the assumptions behind traditional parameterizations are no longer valid
- We review the current efforts by modelers to overcome the gray zone problem in order to provide useful simulations at high resolutions

Correspondence to:
R. Honnert,
rachel.honnert@meteo.fr

The Atmospheric Boundary Layer and the "Gray Zone" of Turbulence: A Critical Review

Rachel Honnert[1], Georgios A. Efstathiou[2], Robert J. Beare[2], Junshi Ito[3], Adrian Lock[4], Roel Neggers[5], Robert S. Plant[6], Hyeyum Hailey Shin[7], Lorenzo Tomassini[4], and Bowen Zhou[8]

[1]Météo-France, CNRM-CNRS UMR-3589, Toulouse, France, [2]Department of Mathematics, University of Exeter, Exeter, UK, [3]Department of Geophysics, Graduate School of Science, Tohoku University, Sendai, Japan, [4]Met Office, UK, [5]Institute for Geophysics and Meteorology, University of Cologne, Cologne, Germany, [6]Department of Meteorology, University of Reading, Reading, UK, [7]National Center for Atmospheric Research, Boulder, CO, USA, [8]Key Laboratory for Mesoscale Severe Weather/MOE and School of Atmospheric Sciences, Nanjing University, Nanjing, China

Abstract Recent increases in computing power mean that atmospheric models for numerical weather prediction are now able to operate at grid spacings of the order of a few hundred meters, comparable to the dominant turbulence length scales in the atmospheric boundary layer. As a result, models are starting to partially resolve the coherent overturning structures in the boundary layer. In this resolution regime, the so-called boundary layer "gray zone," neither the techniques of high-resolution atmospheric modeling (a few tens of meters resolution) nor those of traditional meteorological models (a few kilometers resolution) are appropriate because fundamental assumptions behind the parameterizations are violated. Nonetheless, model simulations in this regime may remain highly useful. In this paper, a newly formed gray zone boundary layer community lays the basis for parameterizing gray zone turbulence, identifies the challenges in high-resolution atmospheric modeling and presents different gray zone boundary layer models. We discuss both the successful applications and the limitations of current parameterization approaches, and consider various issues in extending promising research approaches into use for numerical weather prediction. The ultimate goal of the research is the development of unified boundary layer parameterizations valid across all scales.

1. Introduction

1.1. Boundary Layer Turbulence

The atmospheric boundary layer (ABL) occupies the lowest part of the atmosphere, where most human activities take place and where weather phenomena have significant impacts on the anthropogenic and natural environment. The ABL is in direct contact with the surface and responds to surface forcings on a time scale of about an hour (Stull, 1988). In contrast to the free troposphere, which is located immediately above, the ABL is readily identified by its highly turbulent nature, which is driven by its constant interaction with the surface. Heat, moisture, momentum, and contaminants are transferred and mixed by turbulent eddies having a variety of scales, ranging from a few meters to kilometers. Only under extremely stable conditions, when surface cooling is very strong and winds are very light, does turbulence cease in the ABL.

Turbulent eddies dominate the atmospheric microscales (cf. Orlanski, 1975). They are associated with various atmospheric phenomena such as strong gusts, pollutant dispersion, frost, and fog that have significant social and economical impacts. The largest turbulent structures have scales on the order of the ABL height (about 1–3 km), while the smallest structures are dissipated at a few millimeters.

The convective ABL (CBL) commonly occurs during daytime over continental land, and is characterized by a surface that is warm compared to the air immediately above, resulting in strong surface heat fluxes. Such fluxes give rise to buoyant updraft motions, similar to warm Rayleigh-Bénard structures, called thermals, which are convective eddies extending from the surface to the top of CBL. They are associated with the peak of the energy containing scales shown in Figure 1. The thermals are transitory structures that can move as they evolve. They break up to form smaller eddies so that their energy cascades from scale to scale through a continuous spectrum of eddy size called the "inertial subrange" of turbulence until the Kolmogorov scale is reached and the energy is dissipated (cf. Figure 1).
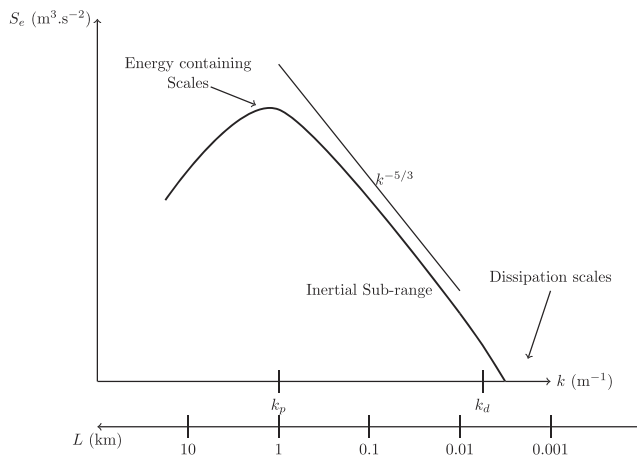
Figure 1. A schematic diagram of the turbulent kinetic energy in the CBL, plotted as a log-log graph as a function of scale. The spectral density of turbulent energy (S_e) is shown as a function of wave number k, and of the corresponding length scale $l = 2\pi/k$.

Supplementing the thermal production of turbulence, mechanical production of turbulence results from the wind shear in the ABL (e.g., due to the fact that wind "vanishes" at the surface), and this can also affect the structure and turbulent transfer in the ABL. Wind shear affects the boundary layer thermals, tilting them or weakening them. Under conditions when the wind is strong or the temperature flows are small (e.g., in the early morning), boundary layer thermals may be organized into convective rolls or cloud streets, which are quasilinear two-dimensional structures (Young et al., 2002). However, under strong surface heating and light winds a regime of *free convection* occurs in the CBL with thermals dominating the transfers of heat, momentum, and moisture from the surface to the overlying ABL and thence to the free troposphere.

The convection inside the CBL is often dry, with no latent heat release within the updrafts. However, if the moisture content is sufficient then shallow clouds (cumulus or stratocumulus) may appear at the top of the ABL where thermals reach their lifting condensation level. Deep moist convection refers to coherent turbulent motions of moist air well into the troposphere and the development of associated deep clouds such as cumulus congestus or cumulonimbus. Although shallow clouds at the top of the ABL will be of interest here, we do not discuss deep clouds in any detail, excepting in so far as we may be concerned with ensuring the appropriate interactions with initiating motions from ABL turbulence.

1.2. Turbulence Modeling and the Terra Incognita

Traditionally, global models of the atmosphere use grid lengths on the order of 10 km or more, but limited-area mesoscale forecasting models may use grid lengths as low as 1 km. Thus, turbulent eddies are usually filtered out from meteorological models and the impact of turbulent transfer on the larger scale flow is parameterized through the use of boundary layer or turbulence schemes.

For modeling at relatively coarse grid lengths, which are larger than the scales of the largest eddies, the turbulence is entirely subgrid (or filtered). The corresponding ABL parameterization schemes are designed to handle 1-D vertical turbulent transfers that arise from the effects of the full spectrum of unresolved turbulent eddies. An additional shallow convection scheme may be needed to parameterize associated shallow cumulus clouds (cf. Section 3.4).

Modeling at fine grid lengths of O(10 m) occupies the regime of large-eddy simulation (LES), where models are able to resolve explicitly most of the turbulent motions. More specifically, simulations may be considered to be LES when the grid length is substantially smaller than the dominant turbulence length scales (i.e., $l_p = 2\pi/k_p$ in Figure 1). Subgrid turbulence is considered to be isotropic when the grid scale lies within the inertial subrange (Figure 1) and the dominant turbulence length scales become very well resolved on the numerical grid (see, e.g., Sullivan & Patton, 2011). At these resolutions subgrid turbulent transfers are therefore 3-D and the role of the subgrid parameterization is to take account of the transfer of energy from the smallest resolved scale to the dissipation scales (k_d) across a clearly defined inertial subrange.

The advance of atmospheric modeling from its infancy in the 1950s to its widespread operational use today has been strongly related to the increase of available computer power. In particular, the development of high performance supercomputers has led to a significant increase of the horizontal grid resolution in numerical weather prediction (NWP). As resolution becomes finer, models start to resolve deep convective clouds. Weather centers around the world are now using high-resolution regional models for weather prediction or climate purposes. The U.K. Met Office runs its U.K. variable resolution model (UKV) with a 1.5 km grid length over the British Isles (Lean et al., 2008), while Météo-France uses the AROME-France convective scale model at 1.3 km (Seity et al., 2011) alongside an ensemble system at 2.5 km (Raynaud & Bouttier, 2017). In the convection-allowing regime, deep convective structures become partially resolved and no longer occupy small fractional areas of the grid. Therefore, the use of conventional deep convective parameterizations at these resolutions becomes highly questionable and they are often switched off.

Pushing toward higher resolutions with grid lengths of O(100 m), atmospheric models become able to partially resolve the largest turbulent structures in the ABL, such as the strong thermals in the CBL. Recent

attempts to run such high-resolution atmospheric models for weather prediction applications include the Météo-France 500 m grid length AROME-airport (Hagelin et al., 2014) run in 2014 for the Single European Sky Air Traffic Research project and the U.K. Met Office 333 m "London model" (Boutle et al., 2015), which was operational for the 2012 London Olympics. Environment-Canada simulated the urban climate of Vancouver using a grid length of 250 m during the Vancouver 2010 Olympic and Paralympic Games (Leroyer et al., 2011).

Wyngaard (2004) first identified that when the size of the largest turbulence structures in the ABL is comparable to the model grid spacing, the fundamental assumptions behind conventional turbulence parameterizations are violated. He named this resolution regime the *terra incognita*, and the concept broadened to become the *gray zone* of turbulence in the mesoscale modeling community, focusing on the convective boundary layer. In the CBL gray zone, the turbulence kinetic energy (TKE) is only partially resolved, in contrast to the LES resolution regime where it is mostly resolved and in contrast to the mesoscale regime where it is fully parameterized.

This paper is organized as follows. Section 2 describes the different facets of the gray zone of turbulence and the related modeling problems. In Section 3 we present the possible solutions that have been proposed in the literature so far, followed by a discussion in Section 4. Conclusions are provided in Section 5.

## 2. Characteristics and Challenges of the Gray Zone of turbulence

2.1. Definition of the Gray Zone of Turbulence

Wyngaard (2004) first studied the terra incognita using near-surface observational data from the Horizontal Array Turbulence Study (HATS) program. The purpose of the HATS field program was to study the interaction between two scales of turbulence (resolved/filtered and subgrid/subfiltered), with the ultimate goal being the improvement of LES parameterizations. The experimental setting consisted of two horizontal crosswind lines of sonic anemometers at two different levels. The filter operation was a filter in time, with Taylor's frozen-turbulence hypothesis being applied to convert to an equivalent spatial filter.

Wyngaard (2004) defined the "terra incognita" at $l \approx \Delta$, where l represents the dominant turbulence length scale and Δ represents the filter length scale. When considered in terms of a numerical model, the filter length must be interpreted as an effective resolution rather than the grid length directly (e.g., Ricard et al., 2013; Skamarock, 2004). The effective resolution depends on the internal diffusion of the model. For instance, a very diffusive atmospheric model may fail to resolve ABL turbulence even at hectometric grid size Δx, if its effective resolution Δ exceeds l.

Inspired by the pioneering work of Wyngaard (2004), Honnert et al. (2011) studied the characteristics of the CBL gray zone by averaging (coarse-graining) LES data from a number of well-documented case studies: the International H_2O project (Couvreux et al., 2005), the Wangara campaign (Clarke et al., 1971), the African Monsoon Multidisciplinary Analysis field campaign (Redelsperger et al., 2006), the Barbados Oceanographic and Meteorological EXperiment (Siebesma et al., 2004), and the ARMCu case (Brown et al., 2002) (cf. Figure 2). The use of HATS data constrained Wyngaard's 2004 analyses to the surface layer, but the use of LES allows the gray zone of turbulence to be studied at higher levels throughout the ABL. The disadvantage is that results may become sensitive to the quality of the LES. Honnert et al. (2011) used LES data as a reference to document the transition of TKE and turbulent fluxes from the LES regime through the CBL gray zone and into the mesoscale regime. Coarse graining of the turbulent structures in the LES data produces smoother fields at hectometric scales in the CBL gray zone until the turbulent variability becomes completely subgrid scale at the mesoscale.

Figure 2 presents horizontal cross sections of vertical velocity at 500 m altitude (in the middle of the ABL) at different horizontal scales ranging from 62.5 m (the LES data) up to 8 km. This example was produced by coarse graining an LES data set based on the International H_2O observational campaign (Weckwerth et al., 2004) using the Méso-NH model (Lac et al., 2018; Lafore et al., 1998). In this example, the transition between the CBL gray zone and the mesoscale occurs at around the 2 km scale, at which some weak turbulent structure can be seen. Honnert et al. (2011) demonstrate that the transition depends on the quantity under consideration: Turbulent structures in the water vapor-mixing ratio field occur on larger scales than those associated with the vertical velocity, in agreement with De Roode et al. (2004).
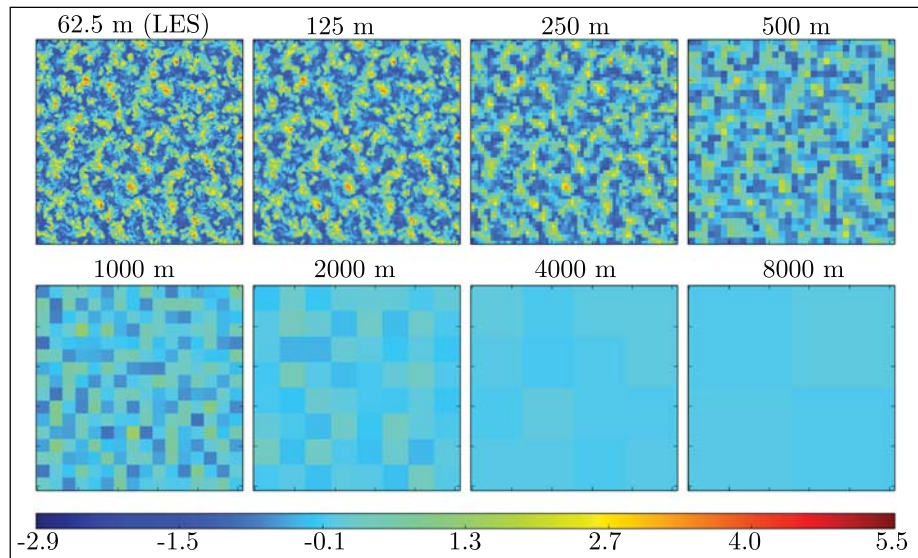
Figure 2. Horizontal cross section of LES vertical velocity data at 500 m altitude (top left) and coarse graining of that data onto a range of scales up to 8 km. The units are m s^{-1}. Adapted from Honnert et al. (2011).

Honnert et al. (2011) considered the largest turbulence length scales l in the CBL to be represented by the sum of the ABL height z_i and the depth of the shallow cloud layer z_c. The basic idea is that the horizontal size of the largest structures is closely linked to their vertical extent. According to this scaling, Honnert et al. (2011) found the CBL gray zone to extend between filter scales of $0.2(z_i + z_c)$ to $2(z_i + z_c)$.

A complementary perspective is provided by Beare (2014), who defines an effective length scale for numerical models, which accounts for the modeled energy dissipation emerging from both the discretized advection and the subgrid schemes. Specifically, the effective dissipation length scale $l_{d,\text{eff}}$ is given by $l_{d,\text{eff}} = 2\pi/k_{d,\text{eff}}$, where

$$k_{d,\text{eff}}^2 = \frac{\int_{k_0}^{k_1} k^2 S_e(k) dk}{\int_{k_0}^{k_1} S_e(k) dk} \tag{1}$$

The k is the wave number and S_e is the TKE power spectrum. Beare (2014) considers a CBL gray zone simulation to be one in which there is no clear separation between the production length scales and the model dissipation scale. In other words, there is no inertial subrange in the model: recall Figure 1. A similarity relationship as a function of $z_i/l_{d,\text{eff}}$ expresses the relative impact of the modeled dissipation scales on the physical production and can be used as a definition for the CBL gray zone. Beare (2014) identifies the transition between the CBL gray zone and the mesoscale regime as occurring at $z_i/l_{d,\text{eff}} = 0.7$.

Figure 3 summarizes the different resolution regimes in atmospheric simulations based on the above and other related studies. The CBL gray zone transition is determined by the dissipation length scale analysis of Equation 1 from Beare (2014), while the LES transition is identified based on the findings of Sullivan and Patton (2011). Between the mesoscale and LES limits, we identify both a *gray zone* and a *near gray zone* (see Efstathiou et al., 2018). In the latter regime, most of the TKE is resolved ($e_{\text{res}}/e_{\text{tot}} \gg 0.5$) but the simulations should not be considered as LES converging because the grid length is not fine enough to present a clear inertial subrange (see also Sullivan & Patton, 2011). The regime might also be thought of as a coarse LES simulation and most practical applications treat the regime similarly to a standard LES. However, such a treatment can have significant implications, especially in cases where the turbulence length scales are evolving (Efstathiou et al., 2018). Taking $l \approx z_i$ and $z_i \approx 1,000$ m, we find that LES converging simulations can be achieved at $\Delta x \sim 20$ m while the CBL gray zone is roughly at 2 km $> \Delta x >$ 200 m.

2.2. Where is the "Truth"?

Turbulent motions are chaotic by definition. Turbulence modeling does not attempt to describe them in full detail but introduces a statistical description of the turbulence. Traditionally, NWP models simulate the
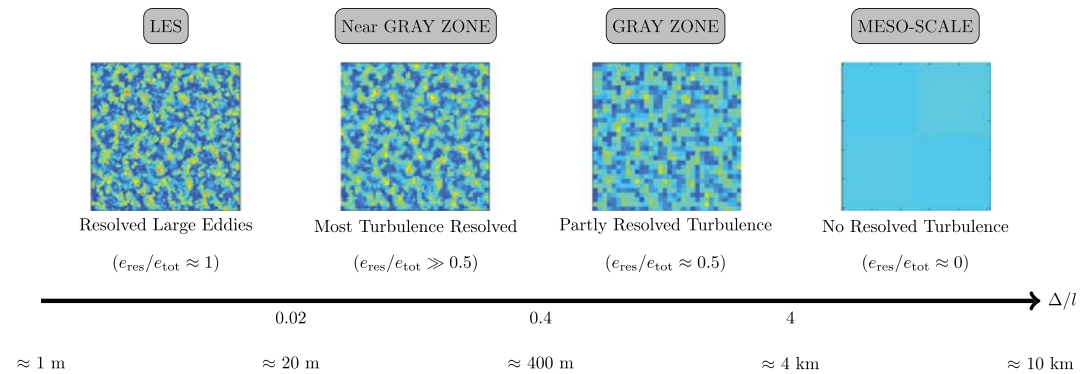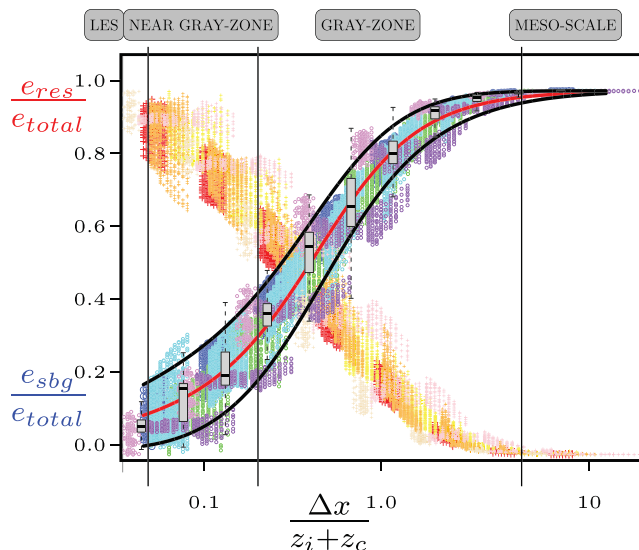
Figure 3. Schematic description of simulation regimes as a function of Δ/l, where Δ is the filter scale and l is the scale of the energy containing structures. Also shown is an estimate of typical model grid spacings. The horizontal cross sections are taken from Figure 2.

Navier-Stokes equations subject to an averaging or filtering operation. The mean quantities after filtering ($\bar{f}$) are often interpreted as representing the most probable state of the atmosphere assuming that the distribution of possible subfilter states is reasonably regular. Turbulence parameterizations for such models are often based on an ensemble average (Mellor & Yamada, 1982): that is, an average over an infinite number of possible independent realizations of the flow. More generally, the averaging operator is assumed to fulfill Reynolds assumption (Stull, 1988; e.g., $\overline{g\bar{f}} = \bar{g}\bar{f}$, where f and g are functions and $\bar{f}$ denotes the average of f).

An alternative to ensemble averaging is to consider the filtering to be a time or space average. This approach is taken, for instance, when researchers average LES output data in order to characterize turbulent statistics (Couvreux et al., 2010; Siebesma & Cuijpers, 1995; see also sections 2.1 and 2.4) and to develop mesoscale parameterizations (e.g., Rio et al., 2010). If a spatial averaging scale is sufficiently large as to sample many eddies then there is often no practical difference between ensemble and spatial averaging. However, for a grid scale that is hectometric the form of the assumed averaging operator becomes crucial.

Using a space-time filter at scales of the gray zone of turbulence, model output fields should become turbulent, and partially resolved turbulent structures appear (cf. Figure 2). Such outputs represent one possible state of the atmosphere on the filtered scales. Real-scale experimental data represent only one possible state of the atmosphere also, and this would likely differ from the model state even if one were to have a perfect model.

2.3. Transition From Subgrid to Resolved Turbulence

As discussed above, turbulence in the CBL gray zone is partially resolved. Using LES data, the partitioning of turbulent energy into that which is subfilter and that which is resolved can be computed for a given filter. The partition will depend upon the filter scale and the size of the turbulent structures. Honnert et al. (2011) considered such partitions for TKE and turbulent fluxes across the transition from the LES converging regime to the mesoscale limit in cases of free dry and cloudy CBLs. The partition function was scaled using the similarity parameter $\Delta x/(z_i + z_c)$ with Δx being the coarse-graining filter scale. Figure 4 shows such a transition curve for the TKE. The approach has also been extended to other types of ABL (Shin & Hong, 2013).

The transition curve for the partitioning of turbulent quantities across scales has become widely used as a reference tool and a test bed for the development and testing of parameterizations for the CBL gray zone (Boutle et al., 2014; Efstathiou & Beare, 2015; Ito et al., 2015; Malavelle et al., 2014; Shin & Hong, 2015; Shin & Dudhia, 2016).

Honnert et al. (2011) evaluated the behavior of a state-of-the-art mesoscale model (Méso-NH) in the CBL by comparing simulations at

Figure 4. Functions showing the partition of the total TKE e_{total} into resolved (e_{res}) and subgrid (e_{sbg}) parts, as a function of $\Delta x/(z_i + z_c)$ (from Honnert et al., 2011): $e_{\text{res}}/e_{\text{total}}$ is in warm colors and $e_{\text{sbg}}/e_{\text{total}}$ is in cold colors. A similarity relation was found to hold in the CBL at altitudes z between $0.05z_i$ and $0.85z_i$.
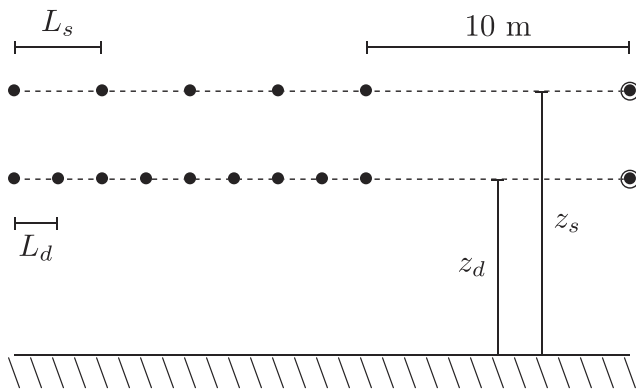
Figure 5. Arrangement of sonic anemometers in the HATS experiments. Single and double arrays are located at heights z_s and z_d above the surface, and the crosswind separation between individual sonic anemometers at each height is L_s and L_d, respectively. Two reference sonic anemometers (circled) are used to monitor the possibility of flow interference among the anemometers in the s and d arrays. Adapted from (Sullivan et al., 2003).

different scales against the reference curve of Figure 4. Within the CBL gray zone, the resolved turbulence was found to be too large when the model's turbulence scheme was used without its mass-flux part. The scheme did not mix the boundary layer efficiently enough, regardless of the mixing length scale parameter that was used within the scheme to calculate the diffusivity. In contrast, Honnert et al. (2011) found the resolved turbulence to be too weak when the mass-flux scheme component of the scheme was activated. This effect strongly depends on the mass-flux scheme (Shin & Dudhia, 2016). One of the mass-flux-type ABL schemes tested in Shin and Dudhia (2016) showed a strong resolved turbulence even though the mass-flux component was activated, because the mass-flux part was not large enough to estimate the vertical transport by strong updrafts.

2.4. Traditional Assumptions of ABL Parameterizations Challenged by the Gray Zone of Turbulence

The results discussed in Section 2.3 illustrate that in the transition between subgrid and resolved turbulence, traditional assumptions made in ABL parameterizations, either at coarse or at very fine resolutions, are no longer valid in the gray zone of turbulence.

Large-scale models assume that the filter length scale (and also the related grid length of the model) is much larger than the important turbulent length scales in the boundary layer and that therefore the representation of turbulence in the boundary layer does not strongly depend on the resolution of the model. They additionally assume, as mentioned in Section 2.2, that turbulent transfer is represented by an ensemble average of all possible flow realizations inside each grid box and as a result only the mean effects of turbulent motion are considered. On the opposite end of the spectrum, LES models require that the inertial subrange is well resolved and so that the subgrid turbulence scheme depends on model resolution in straightforward ways that can be deduced from scaling arguments. In neither case, however, is there any guarantee of an appropriate scale awareness of the subgrid turbulence within the gray zone of turbulence.

Another important issue is that large-scale models assume that subgrid turbulent transport is dominated by the vertical component and are therefore one-dimensional. However, neither is the subgrid turbulence isotropic in three dimensions as commonly assumed by LES models. Thus, the gray zone of turbulence raises issues around the extent of anisotropy.

Wyngaard (2004) rigorously analyzed the turbulent momentum fluxes in the surface ABL with data from an anemometer array. The arrangement is illustrated in Figure 5. He showed that some production terms for turbulent fluxes that may be negligible in the LES and mesoscale limits can nonetheless be significant in the gray zone of turbulence. Such terms are associated with anisotropy of the flow. It is important to bear in mind, however, that the buoyancy-driven turbulence, which dominates in the middle of the CBL is more strongly unidirectional than the shear-driven turbulence which plays an important role in the surface layer.

Honnert and Masson (2014) use LES coarse graining of idealized CBL simulations to assess the scale dependence of turbulence production terms for TKE in the CBL above the surface layer. They show that 3-D dynamical production terms become nonnegligible over flat terrain at resolutions finer than $0.5(z_i + z_c)$, a result which implies that for such scales then 1-D parameterizations do not provide an adequate representation of the TKE. According to Honnert and Masson (2014) the turbulence is anisotropic at about $0.02 \leq \Delta x/(z_i + z_c) \leq 0.5$. This range is consistent with the analysis of (Beare, 2014) for defining the CBL gray zone onset from a different perspective (Section 2.1). Interestingly, Efstathiou and Beare (2015) also related the gray zone onset to the need for different treatments of vertical and horizontal diffusion in their subgrid model when simulating a quasi-steady state CBL.

Moreover, in both large-scale models as well as LES models, subgrid turbulence schemes are usually assumed to be deterministic. Transport in the CBL is characterized by a population of turbulent eddies that cover a range of scales. With increasing model resolution the largest eddies are resolved first. Assuming that a space-time filtering approach is being taken, as in most traditional large-scale models of the ABL, then the part of the eddy size distribution that remains subgrid will become increasingly undersampled, with few of
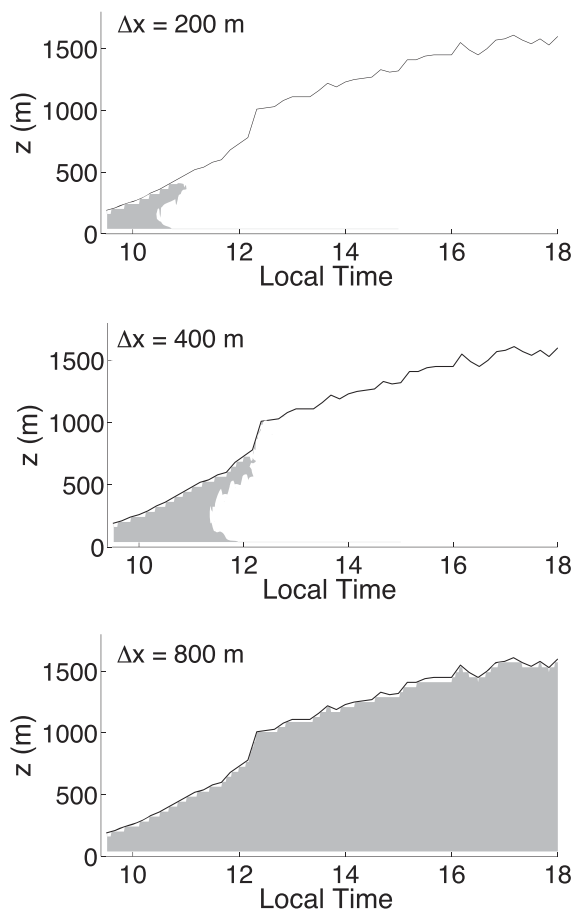
Figure 6. The time evolution of the CBL depth (black line) in a case study simulation of an evolving CBL (Efstathiou et al., 2016) using three different horizontal grid spacings. Shaded in gray color are the parts of the CBL that are considered to be in the gray zone of turbulence according to the analysis of Beare (2014).

the largest unresolved eddies being present on the scale of a grid cell. Thus, one expects to find stochastic behavior near the grid scale in the gray zone of turbulence, and the traditional assumption that the number of eddies or updrafts in each grid cell is large enough to fulfill the "law of large numbers" underlying deterministic parameterizations is no longer valid.

Other important assumptions concern the representation of nonlocal expressions in turbulence parameterizations. These are often formulated using mass-flux approaches (Section 3.4). As resolution increases, the large nonlocal motions will be partially resolved within the CBL gray zone. Mass-flux schemes used in mesoscale models assume that the nonlocal part of the flux is attributable to these CBL thermals, that the resulting flux is stationary, and that the thermals occupy a relatively small area compared to their more quiescent environment. Each model grid cell is supposed to contain both a meaningful number of such thermals and their associated compensatory subsidence. The assumption that the vertical velocity in the grid cell is 0 or that the thermal fraction is negligible breaks down by definition in the CBL gray zone where the thermal length scale is on the order of the grid spacing.

2.5. Gray Zone in an Evolving Convective Boundary Layer

Atmospheric models have a fixed grid length but the turbulence characteristics may change in the course of a simulation. A pertinent example is the development of a CBL that is strongly forced by surface heating, as often occurs over cloud-free land during the morning. Figure 6 shows the evolution of such a developing CBL in a case study using the Met Office Large Eddy Model (LEM) with Δx = 200, 400, and 800 m (Efstathiou et al., 2016). Shaded in gray are the times and heights where the flow is considered to be in the CBL gray zone, according to the analysis of Beare (2014). In the 800 m run the CBL remains in the gray zone throughout the simulation. In contrast, the 200 and 400 m simulations lie in the CBL gray zone only during the early CBL development, albeit with the 400 m run taking somewhat longer to transition to the coarse LES regime. Moreover, near the surface and the top of the ABL the CBL gray zone persists for longer since the turbulent length scales are affected by the presence of these boundaries to the turbulent part of the flow. Thus, we see that a simulated evolving CBL can be in different resolution regimes that can vary both in time and space depending on the scale of the convective structures.

A particular problem in gray zone simulations of an evolving CBL concerns the spin-up of realistic levels of resolved TKE from the initial state. Efstathiou et al. (2016); Zhou et al. (2014) and Kealy et al. (2019) have shown that spin-up is significantly delayed with coarsening resolution within the CBL gray zone. Shin and Hong (2015) also pointed out that their gray zone CBL parameterization delayed the spin-up of resolved motions. The consequence of delayed spin-up is that temperature profiles can become super-adiabatic in response to the lack of nonlocal mixing that the resolved TKE would otherwise provide. Such a delay can also have significant implications when simulating the full diurnal cycle of convection, including the transition from shallow to deep moist convection (e.g., Petch et al., 2002).

2.6. From Shallow to Deep Moist Convection to Synoptic-Scale Systems

Various properties of convective clouds and mesoscale systems in subkilometric models have been demonstrated to be rather sensitive to the choices made in the formulation of turbulent mixing within the gray zone of turbulence. Some good examples can be seen in the idealized modeling studies of Bryan and Morrison (2012), Craig and Dornbrack (2008), Fiori et al. (2010), and Verrelle et al. (2015). Similar case studies in realistic conditions can be found in Bengtsson et al. (2012), Duffourg et al. (2016), Martinet et al. (2017), and Ricard et al. (2013), while a rich statistical perspective is provided by Stein et al. (2015). The studies of Tomassini et al. (2016) and Sakradzija et al. (2016) focus particularly on the interplay between boundary layer turbulence and shallow convective clouds.

The representation of boundary layer turbulence in NWP models does not only interact with (shallow and deep) convective cloud but is also closely interrelated with the representation of the land surface, the atmospheric dynamics, and microphysics (Field et al., 2017). Boundary layer processes are important even for synoptic scale weather systems. In the midlatitudes, boundary layer friction provides a damping mechanism for barotropic vortices through Ekman pumping (Boutle et al., 2015). Baroclinic developments are also dampened by changes to low-level stability, which can be understood in terms of tendencies of potential vorticity that are produced by turbulent mixing processes (Adamson et al., 2006; Stoelinga, 1996). By contrast, in the tropics, boundary layer dynamics may often act to enhance synoptic-scale systems. This is well illustrated by African easterly waves, for which potential vorticity generation by boundary layer processes can feed into the dynamics and contribute to wave growth (Tomassini et al., 2017). Moreover, boundary layer turbulence is important in the establishment of summer time low-level jets over land, which may transport high moist static energy air and feed deep convective development (Chen & Tomassini, 2015). This mechanism is particularly relevant in monsoon regions and at continental-scale precipitation margins.

3. Modeling the ABL in the Gray Zone of Turbulence

As explained in Section 2, the gray zone of turbulence is not a physical phenomenon, but rather, it describes interrelated problems that arise due to the assumptions behind our current turbulence and shallow convection schemes. In this section, we consider some possible solutions that have been proposed to those problems, and their limits.

3.1. Full Transport Model Approach

Wyngaard (2004) suggested using the full transport equations for representing the subgrid scalar transport of a conserved scalar field c at gray zone resolutions in the boundary layer. Without imposing the usual assumptions in mesoscale modeling he introduced a tensor form for the parameterization of the turbulent flux (f_i) of c (see A1 for an outline of the derivation):

$$f_i = -K_{ij} \frac{\partial \bar{c}}{\partial x_j} \tag{2}$$

where K_{ij} is a tensor form of the eddy diffusivity, which is a function of a turbulent time scale, the shear tensor and the Reynolds stress. Thus, Wyngaard's 2004 model can be viewed as a generalized form of the usual diffusion approach which can account for anisotropy of the turbulence. As implied by the arguments of Section 2.4, this extension is an attractive possibility for modeling subgrid fluxes from the LES to the mesoscale limit. The eddy diffusivity is a function of the flow and should be treated as a tensor and not as a scalar. Other elements of the full tensor may become important in the gray zone of turbulence (such as the tilting terms) since the heterogeneity of the convective structures might impose strong horizontal gradients.

Hatlee and Wyngaard (2007) first implemented the approach to study HATS data close to the surface. Kelly et al. (2009) extended the approach to the ocean surface layer by analyzing data from the OHATS (Ocean HATS) observations and developed a simple parameterization for pressure fluctuation induced by moving surface waves. A version of the full transport equations with approximations was implemented by Ramachandran and Wyngaard (2011) in an LES of the convective atmospheric boundary layer. They showed that the anisotropic terms in the subfilter flux equations can indeed become important when the grid length approaches the dominant production scales, in accordance with the HATS analyses of Hatlee and Wyngaard (2007). Therefore, their model produced much better estimations of the momentum and heat fluxes compared to the standard eddy-diffusivity approach.

The full transport model appears to be a promising first approach to modeling in the gray zone of turbulence. Such an approach is expected to behave analogously to a higher-order closure scheme in the mesoscale limit with the appropriate choice of length scales (Wyngaard, 2004). However, the shortage of validation studies, and in particular the absence of a full implementation of the method across the complete range of modeling scales, does not allow firm conclusions to be drawn on the performance or the practical applicability of the scheme.

3.2. TKE Turbulence Modeling

TKE-based turbulence models determine eddy diffusivities based on the magnitude of subgrid TKE, e, specifically,

$$K_c = C_c l_m \sqrt{e} \tag{3}$$

where C_c is a constant which may depend on the variable c of interest, while l_m is the mixing length. l_m may be set using the CBL height in mesoscale models, but is based on the grid spacing in LES applications of the approach. The subgrid TKE itself is obtained by solving its prognostic equation:

$$\frac{\partial \bar{e}}{\partial t} = -\left(\overline{u_i} \frac{\partial \bar{e}}{\partial x_i} + \frac{\partial \overline{u_i' e}}{\partial x_i} + \frac{1}{\rho_0} \overline{u_i' \frac{\partial p'}{\partial x_i}} - \nu \frac{\partial^2 \bar{e}}{\partial x_i^2} \right) - \overline{u_i' u_j'} \frac{\partial \overline{u_j}}{\partial x_i} + \beta \overline{u_3' \theta'} - 2\nu \overline{\left(\frac{\partial u_j'}{\partial x_i} \right)^2} \tag{4}$$

where θ is the potential temperature, p is the pressure, ν is the molecular diffusivity, and β is the buoyancy parameter. Other symbols have been already introduced. The first (in parentheses) term on the right hand side describes the tendency of e due to large-scale advection, turbulence, pressure gradient correlations and molecular diffusion, the second and third terms represent the production of turbulence by wind shear and buoyancy respectively and the last right-hand side term is the dissipation of e.

3.2.1. Pragmatic Approaches Over Complex Terrain

Turbulence parameterizations for atmospheric models have been developed based on assumptions that are, strictly speaking, only valid for horizontally homogeneous and flat terrain and may not be suitable for complex terrain. For example, Monin-Obukhov similarity theory is commonly used to compute surface fluxes and assumes horizontally homogeneous fluxes from the surface into the boundary layer. In complex terrain, Arnold et al. (2012) recommends as a first approach the use of fully prognostic three-dimensional TKE schemes for grid spacings between 100 and 300 m.

Beljaars et al. (2004) proposed a parameterization of turbulent orographic form drag that takes into account the model resolution and is used at ECMWF. However, while there are studies of the behavior of orographic drag in the gray zone of deep convection (5 km resolution) (Sandu, ECMWF Newsletter 150) there are none as yet at the hectometric scales. At hectometric scales, it is not well understood that part of the drag should be taken into account through an explicit parameterization of orographic drag and which part by the turbulence scheme. We note that the model of the Met Office does not include an orographic drag contribution at such scales. Moreover, the theoretical background of the processes involved is not well understood even at mesoscales (see Sandu, ECMWF Newsletter 150). Hence, analysis of the problems in representing orographic drag in the gray zone of turbulence is more difficult than an analysis based on the dynamic production of TKE in the turbulence scheme.

Over complex terrain in the CBL gray zone, the full three-dimensional effects have been found to be important in the shear production term for TKE (Arnold et al., 2014; Goger et al., 2018). Goger et al. (2018) therefore propose an extension of the 1-D prognostic TKE equation used in the COSMO (COnsortium for Small-Scale Modeling) model turbulence scheme because that scheme otherwise underestimates the TKE. The 1-D form considers only the contributions to shear production from vertical gradients of horizontal winds, but Goger et al. (2018) supplement this with a further contribution of

$$\left. \frac{\partial \bar{e}}{\partial t} \right|_{\text{shear}} = (C_s \Delta x)^2 \left[\left(\frac{\partial \bar{u}}{\partial x} \right)^2 + \left(\frac{\partial \bar{v}}{\partial y} \right)^2 + \frac{1}{2} \left(\frac{\partial \bar{u}}{\partial y} + \frac{\partial \bar{v}}{\partial x} \right)^2 \right]^{\frac{3}{2}} \tag{5}$$

where C_s is chosen to be the Smagorinsky constant (see Section 3.3). This extension was tested in simulations over the Alps for a grid length of 1.1 km and had beneficial effects. The verification indicated improvement in the TKE on the slopes, which suggests that the addition of 3D effects is particularly suitable for inclined surfaces.

3.2.2. Adaptive Length Scales

In order to incorporate scale awareness (Section 2.4), various authors have attempted to develop approaches for the gray zone of turbulence that are based on rethinking the mixing length that is used in TKE-based approaches (Equation 3) or other semiempirical length scales used in higher-order turbulence models. Ito et al. (2015), for example, has proposed an extension of Mellor-Yamada-Nakanishi-Niino (MYNN) model for the gray zone of turbulence. The MYNN model is a higher-order turbulence closure designed for 1-D mesoscale applications (Nakanishi & Nino, 2009). The subgrid TKE is predicted using an empirical length scale to parameterize various terms. In the extension the length scale is modified in order to hold the TKE dissipation invariant to the grid resolution. To partition the TKE into appropriate resolved and subgrid contributions, the extension also considers the partition function proposed by Honnert et al. (2011) (as discussed in Section 2.3). Horizontal diffusion based on Ito et al. (2014) is also included in order to take account of

anisotropy (Section 2.4). Ito et al. (2015) showed that a CBL gray zone simulation employing this extension was able to realize reasonable vertical transports.

Kitamura (2015) used a coarse-graining approach on LES data from a CBL simulation in order to estimate the length scale dependence on grid spacing, assuming the form of a TKE-based (Deardorff, 1980) model for the turbulent fluxes. Notably, the estimated length scale was found to depend upon both the horizontal and vertical grid spacings. Kitamura (2016) implemented the resulting mixing length formulations in a modified (Deardorff, 1980) model, which improved the representation of the vertical heat flux and the magnitude of the resolved convection in the CBL gray zone.

Zhang et al. (2018) blended between the subgrid turbulent mixing length scales that are appropriate for the LES and mesoscale limits to create a grid-scale-dependent 3-D TKE scheme. The scheme includes a nonlocal component in the vertical buoyancy, which is also downweighted by a blending function (cf. Boutle et al., 2014) depending on the resolution regime. The blended approach was implemented in WRF and exhibited improved behavior in comparison with a conventional TKE scheme.

Kurowski and Teixeira (2018) also proposed to pragmatically merge the mixing lengths from LES and NWP formulations to obtain a mixing length for intermediate scales:

$$\left(\frac{1}{l_{BL}}\right)^2 = \left(\frac{1}{l_{1D}}\right)^2 + \left(\frac{1}{l_{3D}}\right)^2 + \left(\frac{1}{l_s}\right)^2 \tag{6}$$

where l_{3D} is Deardorff LES mixing length (Deardorff, 1980), l_s is a surface mixing length (see Kurowski & Teixeira, 2018) and l_{1D} is the large-scale NWP mixing length from Teixeira and Cheinet (2004). In their formulation, the mixing length is smaller than the smallest of the three components. Their merged mixing length does not explicitly depend on resolution, but in practice, it increases with increasing grid size until the mesoscales.

3.2.3. Two Turbulence Kinetic Energies

A related approach has been proposed by Bhattacharya and Stevens (2016) who introduce two turbulent kinetic energies in order to distinguish between the energy contained in large eddies spanning the CBL and that within eddies that are subgrid with respect to the vertical grid spacing. The two energies are conceptually linked via the turbulent energy cascade. Bhattacharya and Stevens (2016) formulated distinct length scales to describe mixing and dissipation associated with each energy. However, the problem remains of how to divide the energy due to the boundary layer-scale eddies into resolved and unresolved parts. The approach is yet to be tested in a weather or climate model.

3.3. Extending the Smagorinsky-Lilly Scheme Into the Gray Zone of Turbulence

The Smagorinsky-Lilly (Lilly, 1967; Smagorinsky, 1967) scheme is a widely used standard for LESs of many and various engineering and geophysical flows. Scalar fluxes are represented by

$$f_i = -K_c \frac{\partial \bar{c}}{\partial x_i}, \tag{7}$$

as described in Appendix A (Equation A3). The eddy diffusivity is expressed as

$$K_c = l_t^2 \, |\bar{S}| \, / \, \text{Pr} \tag{8}$$

where Pr is known as the Prandtl number, $|\bar{S}|$ is the modulus of the shear tensor $\bar{S}_{ij} = (\partial \overline{u_i}/\partial x_j) + (\partial \overline{u_j}/\partial x_i)$, and l_t is the turbulence mixing length. The specification is completed by choosing the mixing length to be $l_t = C_s \Delta$ where C_s is known as the Smagorinsky constant. Following the analysis of Lilly (1967) it is often set to 0.17 although different values up to 0.23 have been suggested and used in atmospheric models. The Smagorinsky scheme acts in all three directions with the same eddy diffusivity. Comparing to Equation 2, the scheme is an approximate form of the full turbulent stress tensor model, valid when the full turbulent stress tensor is assumed isotropic, such that $K_{ij} = K_c \delta_{ij}$.

3.3.1. Bounding Approach

Efstathiou and Beare (2015) showed that the standard Smagorinsky scheme becomes too diffusive in the CBL gray zone. Therefore, in order to reduce the over-damping effect arising from the increase in mixing length l_t with horizontal resolution Δx, a modification was made in an attempt to conserve the effective diffusivity of the flow across different grid lengths. As a first approximation, the vertical Smagorinsky diffusivity profile was bounded so that values could not exceed those produced by a 1-D mesoscale approach. The horizontal

diffusion was handled by a 2-D closure and allowed to vary in order to account for anisotropy of the flow at CBL gray zone resolutions. This bounding approach was able to match the energetics of the coarse-grained fields across the transition from the LES to the mesoscale regime in a quasi-steady state CBL.

3.3.2. Dynamic Smagorinsky

The standard Smagorinsky approach is designed for the LES regime and assumes a clear scale separation with the presence of a clear inertial subrange (Section 2.4). The idea behind a dynamic model is to treat C_s as a flow-dependent variable, which can be estimated by comparing the resolved flow against the same flow filtered onto a coarser "test" scale. The idea can also be extended through comparison of the resolved flow against that at two different filtered scales in order to estimate a flow-dependent and scale-dependent C_s. The aim of such a scale-dependent dynamic model is to respect the characteristics of the turbulence spectrum without necessarily requiring the resolved flow to lie within the inertial subrange. Hence, it is a promising extension of Smagorinsky that is well suited to coarse LES resolutions (e.g., Kleissl et al., 2006; Mirocha et al., 2013) and perhaps even to CBL gray zone resolutions.

Efstathiou et al. (2018) modified and implemented a scale-dependent, Lagrangian-averaged dynamic Smagorinsky subgrid scheme based on Bou-Zeid et al. (2005) into the Met Office Large Eddy Model. Extending an earlier study by Basu et al. (2008), they found the approach to perform well for an evolving CBL in capturing the resolved turbulence profiles in comparison with coarse-grained LES fields, especially in the *near gray zone* regime (Figure 3). However, such a dynamic approach reaches a limit of applicability if the test filter is required to sample the flow at a scale for which the turbulence is not adequately represented by the model.

One way around this issue could be the use of the Dynamic Reconstruction Model of Chow et al. (2005), which attempts to reconstruct the smallest resolved scales and uses those to dynamically derive the subgrid mixing length. Simon et al. (2019) tested this approach to simulate a quasi-steady CBL at gray zone resolutions and found significant improvement over conventional schemes and especially compared to the standard Smagorinsky scheme.

3.4. Modifying Boundary Layer 1-D Nonlocal Parameterizations

CBL thermals (cf. Section 2.4) are manifestations of nonlocal turbulence and are responsible for the development of a zone of countergradient fluxes at the top of the CBL, which is ill represented by an eddy diffusivity form (Equation 3).

In mesoscale models, the turbulent transport from the surface to the top of the ABL by convective thermals can be parameterized by the use of an additional countergradient term (Deardorff, 1972) so that

$$f_c = -K_c \left(\frac{\partial \bar{c}}{\partial z} - \gamma \right) \tag{9}$$

where f_c is the turbulent flux of c and γ is the countergradient term. More complex parameterizations have been based on the transilient matrix (Stull, 1984) or the mass-flux scheme (Cheinet, 2003; Hourdin et al., 2002; Pergaud et al., 2009; Rio et al., 2010; Siebesma et al., 2007; Tan et al., 2018). In a mass-flux scheme the turbulent flux is expressed as

$$f_c = -K_c \frac{\partial \bar{c}}{\partial z} + M_u(c_u - \bar{c}) \tag{10}$$

where M_u is the mass-flux associated with the ABL thermals, and c_u is the mean value of c inside the thermals. The second term on the right-hand side represents the transports by coherent thermal plumes whereas the first term is expressed in eddy diffusivity form and represents the contributions from smaller-scale more-localized eddies (Figure 7). This mass-flux approach also lends itself naturally to extensions that treat shallow boundary layer clouds.

Representations of the form of Equations 9 and 10 are designed for mesoscale models, but the split provides an interesting starting point for possible gray zone treatments of turbulence. As resolution increases the large nonlocal motions will be partially resolved within the CBL gray zone for $\Delta \sim z_i$ but the small eddies might remain purely subgrid. With this point in mind, the adaptation of mesoscale models to the CBL gray zone could be achieved by revisiting traditional nonlocal ABL schemes.
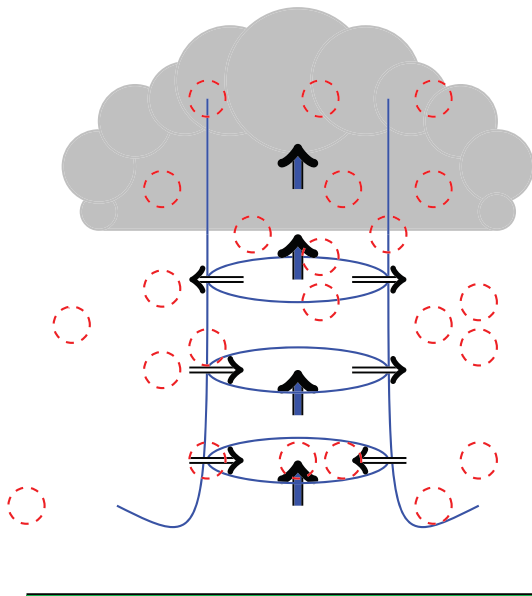
Figure 7. Schematic diagram of small local eddies (red dashed circles), contrasted against a nonlocal thermal (blue tube), which extends from the surface (green) to the cloud layer (in gray).

A mass-flux scheme used at the mesoscales assumes that a nonlocal flux is created by the CBL thermals. This flux is assumed to be stationary and is created by several thermals, which occupy small areas compared to their more quiescent environment. Each model grid cell is supposed to contain both a meaningful number of updrafts and their associated compensatory subsidence. Such assumptions break down by definition in the CBL gray zone where the thermal length scale l is of the order of the grid spacing Δx (Section 2.4). Related issues have been studied in the context of the mass-flux representation of deep convective clouds and are discussed by Arakawa et al. (2011) and Arakawa and Wu (2013), for example.

Honnert et al. (2016) modified a mass-flux scheme for the CBL gray zone (Pergaud et al., 2009), by generalizing the mass-flux equations without the need for assumptions that the vertical velocity in the grid cell is zero or that the thermal fraction is negligible. In this framework, the velocity of the parameterized updraft is reduced when the resolution increases, which then permits the model dynamics to produce resolved structures. The study also incorporates a dependency on the normalized resolution $\Delta x/(z_i + z_c)$ in the surface closure conditions, as discussed further by Lancz et al. (2017).

Shin and Hong (2015) have proposed a one-dimensional parameterization for the CBL gray zone based on Equation 9, but which gradually reduces the parameterized vertical transport as model resolution increases. The local transports from small-scale eddies and the subgrid nonlocal transports are computed separately and reduced at different rates. The nonlocal transport is formulated from three linear profiles which capture its three most important roles: surface layer cooling, mixed-layer heating, and entrainment at the CBL top of air from aloft. Each of these profiles is constructed as a function of stability parameters in the surface and/or entrainment layers. The method is designed to reproduce the total nonlocal turbulent transport, and the required subgrid portion is computed by multiplying an explicit grid size-dependent function, which can also vary according to the transported variable, the height (Honnert et al., 2011), and the stability (Shin & Hong, 2013). The local transport is formulated as an eddy diffusivity and is multiplied by a different grid size-dependent function (Shin & Hong, 2015). Both idealized and real-case simulation results with the CBL gray zone parameterization showed improvements over the use of the conventional unmodified parameterization at CBL gray zone resolutions.

Such changes, however, do not solve all the problems of the gray zone of turbulence. The modified mass-flux, for example, remains based on horizontal homogeneity assumptions. Thus, it should be coupled with a local turbulence scheme that is itself adapted to the CBL gray zone, especially over mountains where it does not produce enough turbulent transports and can lead to unrealistic vertical velocities.

As noted in Section 1.2, the U.K. Met Office runs operational forecasts at gray zone scales of 1.5 km and 333 m. Particularly, in the latter case some of the large eddies responsible for much of the transport are resolved, but other turbulent motions are partially or completely unresolved and continue to require some nonlocal parameterization. The approach has been to devise a pragmatic blending between mesoscale and LES parameterizations (Boutle et al., 2014). The former is provided by the Met Office boundary layer scheme (Lock et al., 2000) (which is similar to Equation 9 for a CBL) and the latter by a 3-D Smagorinsky (Equation 7) scheme. The blending is scale-dependent, being based on the ratio of the grid scale to a diagnosed length scale characterising the turbulence. The benefits of this blended parameterization in the UM are well illustrated by Boutle et al. (2014), where a realistic stratocumulus case was simulated using horizontal grid lengths from 100 m to 1 km, the turbulence changing from largely resolved to largely unresolved. However, the diffusive nature of the Smagorinsky scheme can result in the delayed spin-up of nonlocal motions especially during the handover from the nonlocal mesoscale to the Smagorinsky scheme in deepening CBLs, as shown in Efstathiou et al. (2016). Efstathiou and Plant (2019) extended the blending approach by incorporating a scale-dependent dynamic Smagorinsky scheme instead of the standard static Smagorinsky scheme. They found some promising results in idealized simulations of an evolving CBL, particularly in relation to the spin-up of resolved turbulence (cf. Section 3.3.2).

3.5. The Gray Zone of Turbulence as a Rayleigh-Bénard Convection Problem

Zhou et al. (2014) examined the grid-dependent nature of gray zone CBL simulations using a mesoscale parameterization of turbulence. The analysis is based on the Rayleigh-Bénard (RB) thermal instability framework, with the Rayleigh number (Ra) redefined by its turbulent counterpart

$$Ra = -P_{rT} \frac{N^2 H^4}{\nu_T^2}, \tag{11}$$

where P_{rT} is the turbulent Prandtl number, $N \, (\mathrm{s^{-1}})$ is the buoyancy frequency, $\nu_T \, (\mathrm{m^2 s^{-1}})$ is the eddy viscosity, and H (m) is a length scale over which N is computed. H scales with the boundary layer depth z_i (m). It is set to the surface layer depth (about 0.1 z_i) in Ching et al. (2014), and to z_i in Zhou et al. (2014). In extending the RB analysis to the CBL, the effects of wind shear, which are mostly concentrated in the surface layer and the entrainment zone, are ignored. Turbulent mixing terms are also linearized by assuming an eddy-diffusion representation. Despite its simplicity, the RB framework is useful for understanding model behaviors associated with conventional ABL schemes acting on CBL gray zone grids. For example, the onset of convection in the resolved flow was explained based on the RB framework. The onset depends on a critical value of Ra which is itself a function of grid spacing in the CBL gray zone. Sufficient instability in the surface layer eventually leads to strong grid-scale convection after Ra has reached its critical value.

The turbulent nature of grid-scale convection can mask mesoscale circulations, such as a well-defined sea breeze. Ching et al. (2014) drew on the Rayleigh-Bénard framework to develop a scheme based on the Rayleigh number, which aims to suppress any convective motions in CBL gray zone simulations. Specifically, the thermal diffusivity was modified in order to keep Ra below its critical value and so convective overturning remained as a subfilter process even at very fine grid lengths. This stands in contrast to the other methods discussed in this paper.

3.6. Stochastic Approach

As discussed in Section 2.4, scale adaptive modeling of transport in the boundary layer gray zone is intrinsically linked with representing stochastic behavior. Stochastic backscatter techniques have a well-established value in improving LES simulations close to the Earth's surface. The length scale of the dominant eddies close to the surface is constrained by the presence of the surface, so that $l \sim z$. It follows that the near-surface flow may lie within the turbulence gray zone of $l \sim \Delta$ even for situations in which the turbulence in the interior of the flow is well resolved (Mason & Thomson, 1992; Weinbrecht & Mason, 2008). The backscatter of energy from unresolved scales onto the grid can improve turbulent statistics in such cases and has also proved helpful in the *near gray zone*. A recent extension by O'Neill et al. (2015) allows for grid-independent spatial variations in the backscatter rate.

An important issue in the performance of gray zone turbulence parameterizations, as alluded to several times above, is a mechanism to initiate resolved-scale turbulent structures in an evolving flow. In reality turbulent length scales might be growing from subgrid to resolved scales but as the simulated growth may be overly slow, the explicit inclusion of some local near-grid-scale variability can prove useful. Backscatter, and other stochastic methods, can provide such mechanisms. (An alternative may be to make the low-level temperature profile unrealistically unstable by, for example, suppressing the nonlocal flux, as shown in Efstathiou & Beare, 2015.) The issue is most often discussed in terms of the spin-up of resolved turbulence in time from an initial smooth field. However, similar issues also arise in transitioning to resolved turbulence downstream of the smooth lateral boundary conditions that are usually imposed in NWP. Lateral boundary spin-up has received less attention in the literature to date, but we note that some methods addressing the problem have been developed in the engineering community, involving the injection of synthetic turbulence (e.g., Xie & Castro, 2008), and these ideas may provide a suitable remedy.

Various stochastic parameterization approaches have been developed for climate models and ensemble-based NWP as modifications to mesoscale parameterization methods. To date, these have often been focused on the parameterization of diabatic processes, especially deep convection, and reviews of such techniques are provided by Khouider et al. (2010), Palmer (2012), and Plant et al. (2015). Some of these ideas may also be applied in the CBL gray zone. Simple methods have included rescaling the parameterization tendencies by a random multiplicative factor or making random choices for some of the scheme parameters (Palmer, 2001). Alternatives have attempted to embed stochastic variability at a deeper level, within the subgrid process description. A suitable starting point is to partition the total turbulent flux into contributions

from multiple transporting elements, which may include information about size. Grid-scale adaptivity can then be achieved by size filtering the population (Brast et al., 2018), while stochasticity can be represented in the element properties. A natural choice is to consider that a random number of elements may be found within a grid area (Leoncini et al., 2010; Plant & Craig, 2008), while others allow LES-informed random switching between distinct modes of turbulent heating (Dorrestijn et al., 2013) or random variability in the element/environment mixing rate (Suselj et al., 2014). The variables for which suitable spectra of elements have been constructed include the local thermodynamic state (Cheinet, 2003; Neggers et al., 2002, 2009), the mass-flux carried by the elements (Plant & Craig, 2008; Sakradzija et al., 2014; Sakradzija et al., 2016), or even size itself (Neggers et al., 2019; Park, 2014; Wagner & Graf, 2010).

A simple stochastic method has been implemented operationally in the Met Office UM turbulence-gray zone configurations which draws on some of the above ideas. It can be considered as a simplified stochastic backscatter scheme where random boundary layer temperature and humidity perturbations are applied to the smallest resolvable scale (taken to be eight grid lengths). The magnitude of the perturbations are designed to represent realistic boundary layer variability that would arise from a variety of poorly resolved processes at kilometer scale (not just boundary layer thermals but also surface heterogeneities and convection). The scheme also includes a time correlation of the perturbations on an approximate large-eddy turnover time scale. At present no attempt has been made to make these perturbations scale in a physically appropriate way, for example, with the relative scale of the boundary layer eddies to model resolution. Overall, the scheme gives significant improvements to the initiation of small diurnally triggered convective showers over the United Kingdom and also improves spin-up of convective scale motions from the boundaries. Some other related approaches for introducing physically based boundary layer fluctuations are described by Muñoz-Esparza et al. (2014), Kober and Craig (2016), and Leoncini et al. (2010).

Kealy et al. (2019) examined in more detail the impact of random boundary layer temperature perturbations on the spin-up of resolved turbulence at gray zone resolutions. They found that the combination of imposed perturbations along with a scale-dependent subgrid turbulence scheme has the most pronounced effect on the spin-up of resolved motion.

3.7. Grid Refinement Approach

Zhou et al. (2017) have proposed a rather different modeling methodology for CBL gray zone simulations, based on refining the horizontal grid spacing in the surface layer (the bottom 10–15%). They adopt a two-way nesting technique to couple the simulation of the surface layer with that in the rest of the CBL. Since thermals in the CBL originate from the surface layer, the idea is that an improved representation of the surface layer should induce a good representation of the thermal population throughout the CBL. An LES turbulence closure is used in the surface layer and a mesoscale form of parameterization is adopted aloft. Zhou et al. (2018) demonstrate results which show substantial improvement of first- and second-order turbulent statistics, especially when horizontal resolution is refined up to half of the CBL depth (Zhou et al., 2017).

The grid refinement approach should be considered as a numerical method rather than a parameterization. In the high-resolution surface nest, assumptions behind ABL schemes are completely replaced by traditional LES assumptions (i.e., inertial subrange grid spacing and isotropic subgrid turbulence). The grid refinement method does not really differentiate grid spacings aloft, and can be applied as a general nesting method. The method is of limited use to LES because the turbulent flows are already well resolved in the CBL, although Sullivan et al. (1996) and Huq et al. (2014) did apply a similar method with LES as an improved wall model to better resolve fine-scale surface layer turbulence. The method is also unnecessary for mesoscale models, because however well resolved the thermals are in the nested high-resolution surface grids, they are not expected to have any impact on the coarse mesoscale grids where they are entirely subgrid scale.

3.8. Summary and Critical Review

Section 2 discusses the major challenges of modeling in the CBL gray zone. In the LES regime, the subgrid-scale turbulence is small, homogeneous, and isotropic. At the near gray zone, turbulence starts to become anisotropic (Section 2.4) and the possibility of some resolved-scale turbulence (Section 2.1) is a challenge, not least in producing spin-up problems. In the gray zone regime, the horizontal homogeneity hypothesis, usually used at mesoscales, is no longer valid (Section 2.4) and CBL thermals that are entirely subgrid at the mesoscale (Section 2.2) are partly resolved. Figure 8 summarizes the different regimes and the validity domains of the different parameterizations.
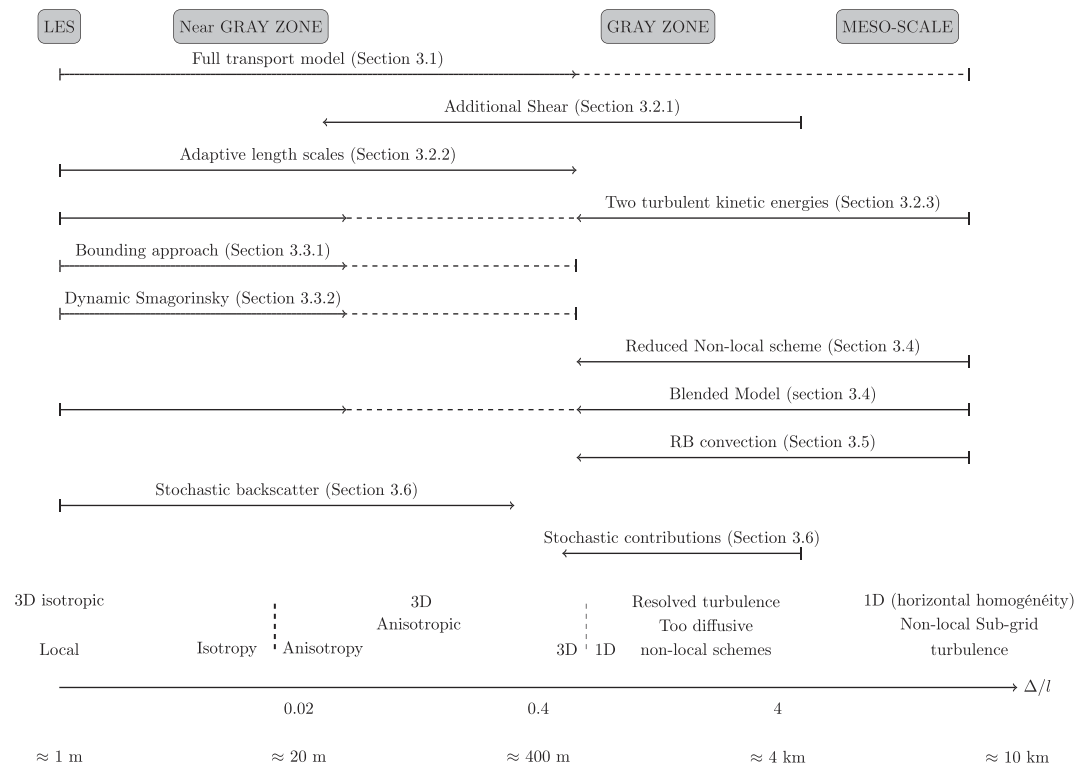
Figure 8. Schematic summarizing the relations between the various approaches that have been introduced and discussed. To simulate the turbulence in the gray zone, each method has a starting point in LES or mesoscale model and to a certain extent gets rid of the initial hypotheses. The dotted line shows where a parameterization family has no theoretical limit, but no application yet.

The experiences of performing CBL gray zone simulations with conventional (LES or mesoscale) parameterizations show that models are likely to fail to capture any resolved turbulence or else to produce unrealistic over-energetic turbulent structures (Honnert et al., 2011). The behavior of models in the gray zone of turbulence depends on various physical factors (surface characteristics, topography, and time of day, among others) and also on the model specifications (such as the grid spacing, the diffusion, numerical damping, etc.). Moreover, the model grid spacing itself can be a poor proxy of the actual model resolution (Ricard et al., 2013; Skamarock, 2004). In particular, the gray zone of turbulence cannot be limited to the hectometric scales: Gray zone issues can impact on modeling at both larger (Goger et al., 2018) and finer scales (Wyngaard, 2004).

Nonetheless, there does seem to be a critical core of new ideas emerging that is well worth pursuing in sub-kilometer simulations. No parameterization is created ex nihilo. Historically, LES and mesoscale schemes have drawn upon assumptions and simplifications that are informed by our understandings of the ABL. For instance, most mesoscale schemes assume that turbulent fluxes are horizontally homogeneous so that only the vertical flux needs to be parameterized. On the other hand, most LES schemes assume that subgrid turbulence is isotropic. The subgrid flux is characterized by a single mixing length when an eddy viscosity model is employed.

Figure 8 shows two categories of scheme. One category treats the gray zone of turbulence by starting from mesoscale approaches and attempt to adapt and extend them for higher resolution applications (mass-flux and counter-gradient schemes modifications (Shin & Hong, 2015), RB representation and most of the stochastic parameterizations). These schemes typically aim to reduce the nonlocal subgrid turbulence but remain focused on a vertical 1-D representation of the CBL. Some of these schemes operate by blending LES and mesoscale formulations, including the two TKE approach (Bhattacharya & Stevens, 2016) and the blended model of Boutle et al. (2014). The blended approaches seem able to produce scale-adapted subgrid CBL thermals, as well as LES isotropic turbulence when necessary. However, there is as yet no good evidence that they can capture the anisotropic character of the turbulence in the near gray zone regime. The

incorporation of additional wind shear terms in a TKE scheme, as in Goger et al. (2018), may compensate for the lack of 3-D turbulence in the gray zone, but it does not produce the limiting forms of behavior of 1-D CBL thermals at the mesoscale or a 3D isotropic scheme in LES. The other major category attempts to treat the gray zone of turbulence as essentially "coarse LES" by adapting and extending LES turbulence models into the gray zone regime (full transport model, all adaptations of the mixing length, bounding model and dynamical Smagorinsky). Such schemes have had some successes, especially in extending from the LES, isotropic, mainly resolved turbulence regime into the near gray zone anisotropic-turbulence region, but they cannot represent nonlocal turbulence typical of the CBL at the mesoscale.

Although most of the parameterizations that have been developed so far cannot be seamlessly used from LES to the mesoscales, they do provide some interesting clues toward solving practical problems in the gray zone of turbulence. Some promising results have emerged from both major categories. Some simple blending/hybrid schemes using nonlocal turbulence (Boutle et al., 2014; Efstathiou & Plant, 2019; Shin & Hong, 2015), TKE (Ito et al., 2015; Zhang et al., 2018), or mass-flux approaches (Honnert et al., 2016) may significantly improve the representation of first-order quantities and turbulence statistics in the CBL gray zone.

4. Discussions

Modeling within the CBL gray zone is increasingly becoming seen as necessary for near future operational use because there is a growing demand for higher resolution forecasting, especially for the prediction of high-impact weather events. A wide range of novel approaches have been presented (Section 3) in this article incorporating various new parameterization ideas to address the challenges of the CBL gray zone. Moreover, an increasing number of researchers are actively working on the topic. Thus, the turbulence gray zone has clearly become a hot topic in atmospheric modeling. However, key questions remain.

4.1. Is the Gray Zone of Turbulence Stalling the Improvement of Atmospheric Modeling?

Our review has shown that most of the gray zone turbulence studies to date have been based on idealized or real but relatively simple well-known cases over homogeneous surfaces (e.g., the Wangara case study). Some caution is therefore needed. In order to develop atmospheric modeling we require not just that there is an appropriate treatment of turbulent motions in the gray zone but also that their treatment should enable the correct interactions with other atmospheric processes. These points are discussed in Section 2.6 and are highlighted by LeMone et al. (2010) or Wagner et al. (2014), for example. However, there are also well-documented cases that clearly benefit from improving resolution into the gray zone of turbulence, despite potential issues with subgrid-scale turbulence parameterization. This can be seen in the simulations of Warren et al. (2014) for a slow-moving organized convective system over a complex terrain area in southwest England.

Most scale-aware gray zone schemes for the CBL have been developed with a focus on cloud-free conditions or with shallow cumulus clouds. It is much less clear how many of the schemes would perform in deep moist convection environments, including organized systems or tropical cyclones. It is also less clear how they might couple to synoptic-scale motions (Section 2.6). A useful study from this perspective is that of Green and Zhang (2015) who investigated the partition between resolved and subgrid turbulent fluxes in turbulence gray zone simulations of hurricane Katrina. In their simulations, the partitioning and the character of the resolved turbulent structures varied significant with the resolution, but the system's intensity was not affected because the total turbulent fluxes remained almost the same. Other case studies of other phenomena with other approaches to the gray zone of turbulence would clearly be valuable.

The complexity of partially resolved structures in the gray zone boundary layer and the feedbacks between resolved and subgrid dynamics during deep convective cloud development are not yet understood. Pronounced sensitivity to turbulent mixing in subkilometer simulations of deep convection has been identified in a number of recent studies. Verrelle et al. (2015) showed that insufficient mixing led to strong undiluted thermals and unrealistic resolved TKE in a super-cell simulation. In Hanley et al. (2014), simulated deep clouds were found to exhibit small features compared to radar observations, although their representation could be somewhat improved by increasing the subgrid turbulence mixing length. Moreover, Verrelle et al. (2017) identified the presence of nonlocal structures in deep clouds that can pose significant challenges to conventional mixing schemes. Ito et al. (2017) examined a number of heavy rainfall cases and found that

the rate of improvement in the skill of the forecasts became progressively smaller for further increases of horizontal resolution into the subkilometric regime. Although their simulations seemed to be relatively insensitive to the CBL representation, the results do indicate that interactions of the near-grid scale with the larger scale environment, and with other processes, might still be important in the gray zone of turbulence.

An important context for these findings is the resolution required for the representation of deep convective clouds. There is a convective gray zone associated with such clouds at grid spacings of around 1–10 km. So-called "convection permitting" simulations with the convection parameterization switched off have been shown to yield some significant benefits for $\Delta x < 5$ km (Roberts & Lean, 2008). However, one would not expect the deep clouds to be well represented on a numerical grid unless one can adequately resolve the turbulent mixing processes at the cloud edges. These have a scale of ~100 m (Craig & Dornbrack, 2008), so improvements in modeling explicit deep convection might prove modest until those grid length scales are reached, *unless* a better parameterization of turbulent mixing processes can be introduced.

As illustrated by Stirling and Petch (2004) and Kealy et al. (2019), the impact of small-scale boundary layer variability is important for an accurate representation of the diurnal cycle of convection in the turbulence gray zone, not least for the timing of deep cloud initiation. This point encourages further development of stochastic approaches and improvement can reasonably be anticipated from imposing appropriate small-scale variability in the CBL.

4.2. Should Resolved Convective Motion be Allowed in the Turbulence Gray Zone?

Ching et al. (2014) argue that any partly resolved turbulent motions in gray zone ABL simulations are not realistic and should be damped. Since the simulations are not in the LES converging regime and the results depend heavily on the imposed dissipation, they should not be trusted. Hence, these authors pursue an ensemble-averaged approach to the model filter operation, in which their gray zone ABL simulations are valued for producing improved numerical accuracy for a mesoscale modeling approach (cf. Mason & Brown, 1999). The authors showed an example of noisy resolved motions that masked the lake-breeze field. However, they do recognize the importance of resolved convective structures in the CBL for the triggering of deep convection, as discussed in the previous subsection.

The initiation of resolved motion in gray zone ABL simulations is generally considered to be a valued aspect for the majority of gray zone ABL studies and for operational atmospheric models. By allowing some partially resolved convective overturning motion, most modelers are (conceptually at least) following a spatially filtered approach in which an *appropriate* level of variability near to the filter scale is considered to be desirable. It should be stressed that this is also the view taken by coarse-graining studies and in simulation strategies developed from those.

4.3. Testing Models in a Realistic Set-up—The Gray Zone Project

The Gray Zone Project promotes international collaborations and community activities in the development of scale-aware deep and shallow convection and boundary layer parameterizations and focuses on grid lengths of about 200 m to 10 km. It has been initiated by WGNE (Working Group on Numerical Experimentation) and the GEWEX (Global Energy and Water Exchanges) Global Atmosphere System Studies.

A first phase of the Gray Zone Project examined the simulation of a maritime cold air outbreak that was observed during a field campaign (Field et al., 2014). Model intercomparisons have been reported for simulations with global models (Tomassini et al., 2016), limited-area models (Field et al., 2017) and LESs (de Roode et al., 2019). Model resolutions were systematically varied in order to explore their behaviors across a range of spatial scales, and results were compared to the observations. A second phase of the project is now being planned and will investigate shallow cumulus clouds at turbulence gray zone resolutions as part of the EUREC4A project in 2020 (Elucidating the role of clouds-circulation coupling in climate; Bony et al., 2017) and also the transition from shallow to deep convective clouds over the eastern tropical Atlantic based on the GATE field campaign (Global Atmospheric Research Program's Atlantic Tropical Experiment; Kuettner, 1974).

4.4. Prognostic Adaptive Schemes the Way Forward?

Most proposed methodologies in the boundary layer gray zone have either LES or mesoscale parameterizations as their starting point. However, various mesoscale parameterizations based on prognostic equations

do exist (e.g., Lappen & Randall, 2001; Tan et al., 2018), and since these tend to be more adaptive to the resolved flow, they may be worth more attention in terms of developing extensions for the gray zone of turbulence. Such mesoscale parameterizations are often designed with an assumption that the thermal fraction is assumed small, which is a defect in the gray zone of turbulence. Modifications such as those in Honnert et al. (2016) to introduce a scale-aware thermal area fraction may therefore be necessary in extending their use. A related starting point could also be that of Thuburn et al. (2018), who recently proposed a two-fluid theoretical framework for the representation of convection in models, using coupled prognostic primitive equations for both the coherent eddy structures (convective plumes) and their environment.

An approach that seems to be able to bridge the gap between the LES and the mesoscale limits is the full transport model of Wyngaard (2004). Nevertheless, solving several prognostic higher-order equations, involving several terms that require further closure assumptions and parameters, can be computationally expensive. Linear algebra closure models such as Lazeroms et al. (2016) could offer a potential route forward to reducing computational costs while retaining the tensor representation of the fluxes that is at the core of the approach. In either case, the dynamic modeling technique of filtering at multiple scales (Bou-Zeid et al., 2005; Chow et al., 2005) can be used to determine the necessary length scales and tuning parameters, thereby making such schemes not only scale-aware but also flow dependent. Dynamic calculation of length scales in an evolving CBL has been shown to be beneficial for the CBL gray zone (Efstathiou et al., 2018; Efstathiou & Plant, 2019).

It is clear that special care needs to be taken in the gray zone of turbulence for the representation of horizontal fluxes Zhou et al. (2017). The conventional 2D Smagorinsky adaptation for horizontal mixing has been shown to be inappropriate in the representation of CBL mixing (Ito et al., 2014; Zhou et al., 2017). A recent scale-aware representation of horizontal diffusion from (Zhang et al., 2018), based on Honnert et al. (2011) and using the blending approach of Boutle et al. (2014), has shown promising results.

5. Conclusions

We have reviewed the current state of a newly emerged research area in the numerical modeling of geophysical flows and discussed the significant challenges that arise for the atmospheric modeling community. Numerical models are now moving toward subkilometer grid spacings at which they produce partially resolved turbulent structures. As a result in the "gray zone" of turbulence, the fundamental assumptions underpinning our conventional treatments of subgrid-scale variability are no longer valid. Furthermore, at CBL gray zone resolutions the resolved-scale variability becomes highly dependent on the representation of subgrid motion that in turn can compromise the accuracy and value of the numerical model simulations.

A model's horizontal grid spacing cannot by itself determine the onset of the CBL gray zone or explain the transition of the TKE and heat and moisture fluxes from the LES to the mesoscale limit. The key to describing the transition is to consider the relative extent of the dominant turbulence length scales compared to the effective grid spacing. This means that different structures, whether these are CBL thermals or clouds at the top of the ABL, might be in different resolution regimes especially as they evolve over time (similar to Figure 6). It also means that one should take into account the imposed dissipation from the numerical methods in use, which can damp or smooth the resolved field. The interplay of numerical and "physical" diffusion (from the turbulence parameterization) will determine the effective resolution of an atmospheric model; that is, its ability to partially resolve features at the limits of its grid resolution (Skamarock, 2004).

The proposed gray zone CBL parameterization schemes in the literature, as presented here, are largely based on two approaches: treating the gray zone of turbulence as either a coarse LES or a high-resolution mesoscale model depending on the starting point of each parameterization. However, there are some approaches that attempt to avoid the bulk of the gray zone of turbulence, either by increasing the horizontal resolution in certain parts of the CBL or by filtering out any turbulent motions. The latter approach considers the simulation to belong the mesoscale resolution regime where all of the turbulent transfer is parameterized in an ensemble-averaged sense. Even though many of the schemes considered show certain merits and benefits in the gray zone of turbulence, most of them have been tested in idealized settings. As a next step more comprehensive studies are needed using realistic case studies to identify the interactions of partially resolved turbulent mixing with deep convective clouds and with the larger-scale circulations.

The full turbulent transfer equations should, at least in principle, be able to handle the transition of turbulent transfer from well resolved to fully parameterized. However, solving the full turbulent transport equations would be computationally expensive and suitable closure assumptions would be needed, perhaps depending on the level of information that is available from the resolved motions. As this approach may not be practical, even with the available computing power, the anisotropic production terms in the transport equations might be usefully retained in various simplified ways.

It is very clear that the existence of the turbulence gray zone has important implications and consequences for atmospheric modeling and for the future of NWP in particular. Recent studies, such as those discussed in Section 4, have demonstrated that at subkilometer grid spacings increasing convergence with increasing grid resolution is not guaranteed, especially in simulations with deep convection. However, the full extent of the impact of partially resolved turbulent flow on the actual performance of weather forecasting models needs to be further investigated. This is partly due to the fact that some of the feedbacks between the turbulent mixing in the CBL and synoptic-scale systems are not yet well understood. Nevertheless, the refined resolution can still prove to be beneficial, especially when it is combined with better representation of topography and surface heterogeneity and especially in cases with strong large-scale forcing.

Although this article has been focused on the CBL gray zone and atmospheric simulations, other aspects of geophysical fluid flow modeling experience their own gray zone. The representation of any important physical phenomenon with a length scale of the same order as the grid spacing is liable to be problematic in numerical simulations. Such a situation is clearly undesirable but sometimes cannot be avoided, due to finite computational limitations or else because the phenomenon itself covers a range of scales. The CBL gray zone is *relatively* simple in various respects, the dominant turbulent structures being well understood and having a well-defined length scale dictated by the CBL depth. Thus, it provides a good base case for the study of possible methods for treating gray zone motions in geophysical flows more generally. Promising approaches to gray zones may be more easily identified in this setting, and conversely, it seems difficult to imagine that approaches performing poorly for the CBL gray zone would somehow work well in other, more complex settings.

Appendix A: The Full Transport Equations

In Section 3.1 a tensor form of the eddy diffusivity was presented. Following (Wyngaard, 2004), this may be derived from the scalar-flux transport equation. The subgrid flux of a conserved scalar field c in the i direction is denoted $f_i = \overline{cu_i} - \bar{c}\,\bar{u}_i$ where the overbar is a spatial filter, and it evolves as (Wyngaard, 2004):

$$\frac{\partial f_i}{\partial t} + \bar{u}_j \frac{\partial f_i}{\partial x_j} = -f_j \frac{\partial \bar{u}_i}{\partial x_j} - \tau_{ij} \frac{\partial \bar{c}}{\partial x_j} + \text{PT} + \text{FLXDIV}, \tag{A1}$$

The first two terms on the right-hand side are production terms, the first (tilting term) representing the stretching and "tilting" of turbulent eddies and the second representing the interaction of turbulent fluxes (Reynolds stresses, τ_{ij}) with the scalar gradient (gradient term). Other terms express the pressure-scalar interactions (PT) and the divergence of the subgrid flux of f_i (FLXDIV). The flux divergence terms contain higher order contributions that express the subgrid turbulent transport of f_i. PT acts as a principal sink for the scalar flux and can be parameterized as $-f_i/T$ in its simplest linear form, with T representing a characteristic time scale of the subgrid turbulence.

Wyngaard (2004) proposed a model for the subgrid scalar fluxes that is obtained by retaining the first two production terms in Equation A1, assuming a steady state, and balancing the production with the pressure terms. The model is given by

$$f_i = -T \left(f_j \frac{\partial \bar{u}_i}{\partial x_j} + \tau_{ij} \frac{\partial \bar{c}}{\partial x_j} \right). \tag{A2}$$

Although Equation A2 expresses an algebraic model, it would be entirely straightforward to retain a prognostic form based on Equation A1.

Dropping the tilting terms and retaining only the gradient production terms in the direction of the flux (isotropic gradient production), Equation A2 reduces to

$$f_i = -T \tau_{ii} \frac{\partial \bar{c}}{\partial x_i} = -K_c \frac{\partial \bar{c}}{\partial x_i}. \tag{A3}$$

This corresponds to the downgradient diffusion model that is commonly used as a basis for turbulence parameterization in both LES closures and mesoscale ABL schemes. $K_c = T\tau_{ii}$ is the eddy diffusivity. Without these additional assumptions, the formal solution of Equation A2 is given by Equation 2 (Wyngaard, 2004):

$$f_i = -K_{ij} \frac{\partial \bar{c}}{\partial x_j} \tag{A4}$$

where K_{ij} is a tensor form of the eddy diffusivity which is a function of T, the shear tensor $\partial \bar{u}_i / \partial x_j$, and τ_{ij}.

Glossary

Atmospheric boundary layer	The bottom layer of the atmosphere that is in contact with the surface of the Earth.
Free troposphere	The part of the Earth's troposphere which excludes the boundary layer. Turbulence in the boundary layer is ubiquitous but in the free troposphere is produced only sporadically, by mechanical forcing in regions of pronounced wind shear or thermally inside convective clouds.
Backscatter	Energy transfers in turbulent three-dimensional fluid motions occur to both larger and smaller spatial scales. The net transfer within the inertial subrange is downscale but the backscatter refers to the upscale component of energy transfer, from subgrid-scale to resolved motions.
Baroclinic waves	Synoptic-scale disturbances that grow in the midlatitudes due to baroclinic instability and which are responsible for the development of weather systems.
Deep clouds	Clouds with predominantly vertical development that form as a result of deep convection in the troposphere. They may extend from the top of the boundary layer toward the upper troposphere (cumulus congestus) or as far as the tropopause (cumulonimbus). Such clouds may be associated with thunderstorms, heavy rainfall, and hail.
LES	A three-dimensional numerical simulation of turbulence, in which the largest eddies are explicitly resolved, while the effects of subgrid-scale eddies in the inertial subrange are parameterized.
Large/synoptic scale	The scales of the general atmospheric circulation related to the high-tropospheric long-wave patterns.
Low-level jet	A jet of wind that appears in the boundary layer.
Mesoscale	Refers to atmospheric phenomena having horizontal scales ranging from a few to several tens of kilometers, including thunderstorms, squall lines, and topographically induced circulations such as mountain waves, mountain, and valley breezes as well as sea and land breezes.
Parameterization	The representation, in a dynamic model, of physical effects in terms of admittedly oversimplified parameters, rather than realistically requiring such effects to be consequences of the dynamics of the system (from American Meteorological Society Glossary).
Shallow clouds	Low-level, usually nonprecipitating, clouds, which may be considered to form part of the ABL. Cumulus and stratocumulus are forms of shallow convective clouds.
Troposphere	That portion of the atmosphere where most weather occurs and which extends from the Earth's surface to a sharp temperature inversion at the tropopause, between 10 and 20 km aloft.
Surface layer	The lowest 10–15% of the ABL where first-order quantities such as wind and temperature follow an approximately logarithmic profile and turbulent fluxes may be considered almost constant.
Nonlocal turbulence	A term used in the context of 1-D mesoscale parameterizations to refer to coherent turbulent structures that typically extend to the full depth of the turbulent layer. In the CBL, nonlocal turbulence is associated with buoyant thermals.

Acronyms

ABL	atmospheric boundary layer
CBL	convective (atmospheric) boundary layer
COSMO	COnsortium for Small-Scale Modeling
GEWEX	Global Energy and Water Exchanges Global
LEM	Met Office Large Eddy Model
LES	large-eddy Simulation
MYNN	Mellor-Yamada-Nakanishi-Niino model
NWP	numerical weather prediction
RB	Rayleigh-Bénard
TKE	turbulent kinetic energy
VLES	very large-eddy simulation
WGNE	Working Group on Numerical Experimentation
WRF	Weather Research and Forecasting

Notation

c	a conserved scalar.
c_u	value of c inside the mass-flux thermal plume
$\bar{c}$	mean value of c
C_c	a constant value for a given scalar c
C_s	Smagorinsky coefficient
Δ	grid spacing, model resolution
Δx	model horizontal grid spacing
Δz	model vertical spacing
e	TKE
e_{sgs}	subgrid-scale TKE
e_{res}	resolved TKE
e_{tot}	total (resolved plus subgrid-scale) TKE
f_i	subgrid scalar flux
γ	countergradient term
H	a length scale over which N is computed
k	wave number
$k_{d,\text{eff}}$	dissipation wave number in Beare (2014)
k_d	dissipation wave number
k_0, k_1	wave number limits in Beare (2014)
K_c	the eddy diffusivity associated with the conserved variable c
K_{ij}	a tensor form of the eddy diffusivity
l	length scale of the dominant energy containing structures
l_m	mixing length used in a TKE based parameterization
l_t	Smagorinsky mixing length scale
l_d	dissipation length scale
ν_T	the eddy viscosity
M_u	mass-flux of ABL thermals
Pr	Prandtl number
P_{rT}	turbulent Prandtl number
Ra	Rayleigh number
τ_{ij}	Reynolds stress
S_e	TKE power spectrum
T	time scale for subgrid turbulence
θ	potential temperature
u	a wind component
w	vertical velocity

z_c depth of the cloud layer
z_i CBL height
z altitude

References

Adamson, D. S., Belcher, S. E., Hoskins, B. J., & Plant, R. S. (2006). Boundary-layer friction in midlatitude cyclones. *Quarterly Journal of the Royal Meteorological Society*, *132*, 101–124.

Arakawa, A., Jung, J.-H., & Wu, C.-M. (2011). Toward unification of the multiscale modeling of the atmosphere. *Atmospheric Chemistry and Physics*, *11*(8), 3731–3742.

Arakawa, A., & Wu, C.-M. (2013). A unified representation of deep moist convection in numerical modeling of the atmosphere. Part I. *Journal of the Atmospheric Sciences*, *70*(7), 1977–1992.

Arnold, D., Morton, D., Schicker, I., Seibert, P., Rotach, M., Horvath, K., et al. (2012). High resolution modelling in complex terrain. Vienna: Report on the HiRCoT 2012 Workshop.

Arnold, D., Morton, D., Schicker, I., Seibert, P., Rotach, M., Horvath, K., et al. (2014). Issues in high-resolution atmospheric modeling in complex terrain—The HiRCoT workshop. *Croatian Meteorological Journal*, *47*, 3–11.

Basu, S., Vinuesa, J.-F., & Swift, A. (2008). Dynamic LES modeling of a diurnal cycle. *Journal of Applied Meteorology and Climatology*, *47*, 1156–1174.

Beare, R. J. (2014). A length scale defining partially-resolved boundary-layer turbulence simulations. *Boundary-Layer Meteorology*, *151*, 39–55.

Beljaars, A. C. M., Brown, A. R., & Wood, N. (2004). A new parametrization of turbulent orographic form drag. *Quarterly Journal of the Royal Meteorological Society*, *130*(599), 1327–1347.

Bengtsson, L., Tijm, S., Vana, F., & Svensson, G. (2012). Impact of flow-dependent horizontal diffusion on resolved convection in AROME. *Journal of Applied Meteorology and Climatology*, *51*(1), 54–67.

Bhattacharya, R., & Stevens, B. (2016). A two turbulence kinetic energy model as a scale adaptive approach to modeling the planetary boundary layer. *Journal of Advances in Modeling Earth Systems*, *8*, 224–243. https://doi.org/10.1002/2015MS000548

Bony, S., Stevens, B., Ament, F., Bigorre, S., Chazette, P., Crewell, S., et al. (2017). EUREC4A: A field campaign to elucidate the couplings between clouds, convection and circulation. *Surveys in Geophysics*, *38*, 1529–1568.

Bou-Zeid, E., Meneveau, C., & Parlange, M. (2005). A scale-dependent Lagrangian dynamic model for large eddy simulation of complex turbulent flows. *Phys Fluids*, *17*(2), 025105. https://doi.org/10.1063/1.1839152

Boutle, I. A., Belcher, S. E., & Plant, R. S. (2015). Friction in mid-latitude cyclones: An Ekman-PV mechanism. *Atmospheric Science Letters*, *16*, 103–109.

Boutle, I. A., Eyre, J. E. J., & Lock, A. P. (2014). Seamless stratocumulus simulation across the turbulent grey zone. *Monthly Weather Review*, *142*, 1655–1668.

Brast, M., Schemann, V., & Neggers, R. A. J. (2018). Investigating the scale-adaptivity of a size-filtered mass flux parameterization in the gray zone of shallow cumulus convection. *Journal of the Atmospheric Sciences*, *75*, 1195–1214.

Brown, A. R., Cederwall, R. T., Chlond, A., Duynkerke, P. G., Golaz, J.-C., Khairoutdinov, M., et al. (2002). Large-eddy simulation of the diurnal cycle of shallow cumulus convection over land. *Quarterly Journal of the Royal Meteorological Society*, *128*, 1075–1093.

Bryan, G. H., & Morrison, H. (2012). Sensitivity of a simulated squall line to horizontal resolution and parameterization of microphysics. *Monthly Weather Review*, *140*, 202–225.

Cheinet, S. (2003). A multiple mass-flux parameterization for the surface-generated convection. Part I: Dry plumes. *Journal of the Atmospheric Sciences*, *60*, 2313–2327.

Chen, R., & Tomassini, L. (2015). The role of moisture in summertime low-level jet formation and associated rainfall over the East Asian monsoon region. *Journal of the Atmospheric Sciences*, *72*, 3871–3890.

Ching, J., Rotunno, R., LeMone, M., Martilli, A., Kosovic, B., Jimenez, P. A., & Dudhia, J. (2014). Convectively induced secondary circulations in fine-grid mesoscale numerical weather prediction models. *Monthly Weather Review*, *142*(9), 3284–3302.

Chow, F. K., Street, R. L., Xue, M., & Ferziger, J. H. (2005). Explicit filtering and reconstruction turbulence modeling for large-eddy simulation of neutral boundary layer flow. *Journal of the Atmospheric Sciences*, *62*(7), 2058–2077. https://doi.org/10.1175/JAS3456.1

Clarke, R. H., Dyer, A. J., Reid, D. G., & Troup, A. J. (1971). *The Wangara experiment: Boundary layer data* (Vol. 19). Australia: Division Meteorological Physics Paper, CSIRO.

Couvreux, F., Guichard, F., Redelsperger, J.-L., Kiemle, C., Masson, V., Lafore, J.-P., & Flamant, C. (2005). Water vapour variability within a convective boundary-layer assessed by large-eddy simulations and IHOP2002 observations. *Quarterly Journal of the Royal Meteorological Society*, *131*, 2665–2693.

Couvreux, F., Hourdin, F., & Rio, C. (2010). Resolved versus parametrized boundary-layer plumes. Part I: A parametrization-oriented conditional sampling in large-eddy simulations. *Boundary-layer Meteorol*, *134*(3), 441–458.

Craig, G. C., & Dornbrack, A. (2008). Entrainment in cumulus clouds: What resolution is cloud-resolving? *Journal of the Atmospheric Sciences*, *65*, 3978–3988.

De Roode, S. R., Duynkerke, P. G., & Jonker, H. J. J. (2004). Large-eddy simulation: How large is large enough? *Journal of the Atmospheric Sciences*, *61*, 403–421.

de Roode, S. R., Frederikse, T., Siebesma, A. P., Ackerman, A. S., Field, P. R., Hill, A., et al. (2019). Turbulent transport in the grey zone: A large-eddy simulation intercomparison study of the CONSTRAIN cold air outbreak case. *Journal of Advances in Modeling Earth Systems*, *11*, 597–623.

Deardorff, J. W. (1972). Theoretical expression for the counter gradient vertical flux. *Journal of Geophysical Research*, *77*(30), 5900–5904.

Deardorff, J. W. (1980). Stratocumulus-capped mixed layers derived from a three-dimensional model. *Boundary-Layer Meteorology*, *18*, 495–527.

Dorrestijn, J., Crommelin, D. T., Siebesma, A. P., & Jonker, H. J. J. (2013). Stochastic parameterization of shallow cumulus convection estimated from high-resolution model data. *Theoretical and Computational Fluid Dynamics*, *27*(1-2), 133–148. https://doi.org/10.1007/s00162-012-0281-y

Duffourg, F., Nuissier, O., Ducrocq, V., Flamant, C., Chazette, P., Delanoé, J., et al. (2016). Offshore deep convection initiation and maintenance during HyMeX IOP16a heavy precipitation event. *Quarterly Journal of the Royal Meteorological Society*, *142*, 259–274.

Efstathiou, G. A., & Beare, R. J. (2015). Quantifying and improving sub-grid diffusion in the boundary-layer grey zone. *Quarterly Journal of the Royal Meteorological Society*, *141*(693), 3006–3017.

Efstathiou, G. A., Beare, R. J., Osborne, S., & Lock., A. P. (2016). Grey zone simulations of the morning convective boundary layer development. *Journal of Geophysical Research: Atmospheres*, *121*, 4769–4782. https://doi.org/10.1002/2016JD024860

Efstathiou, G. A., & Plant, R. S. (2019). A dynamic extension of the pragmatic blending scheme for scale-dependent sub-grid mixing. *Quarterly Journal of the Royal Meteorological Society*, *145*, 884–892.

Efstathiou, G. A., Plant, R. S., & Bopape, M. M. (2018). Simulation of an evolving convective boundary layer using a scale-dependent dynamic Smagorinsky model at near-gray-zone resolutions. *Journal of Applied Meteorology and Climatology*, *57*, 2197–2214.

Field, P. R., Brozkov, R., Chen, M., Dudhia, J., Lac, C., Hara, T., et al. (2017). Exploring the convective grey zone with regional simulations of a cold air outbreak. *Quarterly Journal of the Royal Meteorological Society*, *143*(707), 2537–2555. https://doi.org/10.1002/qj.3105

Field, P. R., Cotton, R. J., McBeath, K., Lock, A. P., Webster, S., & Allan, R. P. (2014). Improving a convection-permitting model simulation of a cold air outbreak. *Quarterly Journal of the Royal Meteorological Society*, *140*, 124–138.

Fiori, E., Parodi, A., & Siccardi, F. (2010). Turbulence closure parameterization and grid spacing effects in simulated supercell storms. *Journal of the Atmospheric Sciences*, *67*(12), 3870–3890.

Goger, B., Rotach, M. W., Gohm, A., Fuhrer, O., Stiperski, I., & Holtslag, A. A. M. (2018). The impact of three-dimensional effects on the simulation of turbulence kinetic energy in a major Alpine valley. *Boundary-Layer Meteorology*, *168*(1), 1–27.

Green, B. W., & Zhang, F. (2015). Numerical simulations of Hurricane Katrina (2005) in the turbulent gray zone. *Journal of Advances in Modeling Earth Systems*, *7*, 142–161. https://doi.org/10.1002/2014MS000399

Hagelin, S., Auger, L., Brovelli, P., & Dupont, O. (2014). Nowcasting with the AROME model: First results from the high-resolution AROME airport. *Weath and Forecasting*, *29*, 773–787.

Hanley, K. E., Plant, R. S., Stein, T. H. M., Hogan, R. J., Nicol, J. C., Lean, H. W., et al. (2014). Mixing-length controls on high-resolution simulations of convective storms. *Quarterly Journal of the Royal Meteorological Society*, *141*(686), 272–284. https://doi.org/10.1002/qj.2356

Hatlee, S. C., & Wyngaard, J. C. (2007). Improved subfilter-scale models from the HATS field data. *Journal of the Atmospheric Sciences*, *64*, 1694–1705.

Honnert, R., Couvreux, F., Masson, V., & Lancz, D. (2016). Sampling of the structure of turbulence: Implications for parameterizations at sub-kilometric scales. *Boundary-Layer Meteorology*, *2:27*. https://doi.org/10.3389/feart.2014.00027

Honnert, R., & Masson, V. (2014). What is the smallest physically acceptable scale for 1d turbulence schemes? *Frontiers in Earth Science*, *2*, 27. https://doi.org/10.3389/feart.2014.00027

Honnert, R., Masson, V., & Couvreux, F. (2011). A diagnostic for evaluating the representation of turbulence in atmospheric models at the kilometric scale. *Journal of the Atmospheric Sciences*, *68*, 3112–3131.

Hourdin, F., Couvreux, F., & Menut, L. (2002). Parameterization of the dry convective boundary layer based on a mass flux representation of thermals. *Journal of the Atmospheric Sciences*, *59*, 1105–1122.

Huq, S., De Roo, F., Raasch, S., & Mauder, M. (2014). Vertical grid nesting for improved surface layer resolution in large-eddy simulation. In *21st Symposium on Boundary Layers and Turbulence*.

Ito, J., Hayashi, S., Hashimoto, A., Ohtake, H., Uno, F., Yoshimura, H., et al. (2017). Stalled improvement in a numerical weather prediction model as horizontal resolution increases to the sub-kilometer scale. *SOLA*, *13*, 151–156. https://doi.org/10.2151/sola.2017-028

Ito, J., Niino, H., & Nakanishi, M. (2014). Horizontal turbulent diffusion in a convective mixed layer. *Journal of Fluid Mechanics*, *758*, 553–564. https://doi.org/10.1017/jfm.2014.545

Ito, J., Niino, H., Nakanishi, M., & Moeng, C-H. (2015). An extension of Mellor-Yamada model to the terra incognita zone for dry convective mixed layers in the free convection regime. *Boundary-Layer Meteorology*, *157*(1), 23–43.

Kealy, J., Efstathiou, G. A., & Beare, R. J. (2019). The onset of resolved boundary-layer turbulence at grey-zone resolutions. *Boundary-Layer Meteorology*, *171*, 31–52.

Kelly, M., Wyngaard, J. C., & Sullivan, P. P. (2009). Application of a subfilter-scale flux model over the ocean using OHATS field data. *Journal of the Atmospheric Sciences*, *66*(10), 3217–3225.

Khouider, B., Biello, J., & Majda, A. J. (2010). A stochastic multicloud model for tropical convection. *Communications in Mathematical Sciences*, *8*, 187–216.

Kitamura, Y. (2015). Estimating dependence of the turbulent length scales on model resolution based on a priori analysis. *Journal of the Atmospheric Sciences*, *72*, 750–762.

Kitamura, Y. (2016). Application of the new turbulence length scale for the terra incognita range to numerical simulations of a convective boundary layer. *Journal of the Meteorological Society of Japan*, *94*, 491–506.

Kleissl, J., Kumar, V., Meneveau, C., & Parlange, M. B. (2006). Numerical study of dynamic Smagorinsky models in large-eddy simulation of the atmospheric boundary layer: Validation in stable and unstable conditions. *Water Resources Research*, *42*, W06D10. https://doi.org/10.1029/2005WR004685

Kober, K., & Craig, G. C. (2016). Physically based stochastic perturbations (PSP) in the boundary layer to represent uncertainty in convective initiation. *Journal of the Atmospheric Sciences*, *73*, 2893–2911.

Kuettner, J. P. (1974). General description and central program of GATE. *Bulletin of the American Meteorological Society*, *55*, 712–719.

Kurowski, M. J., & Teixeira, J. (2018). A scale-adaptive turbulent kinetic energy closure for the dry convective boundary layer. *Journal of the Atmospheric Sciences*, *75*(2), 675–690.

Lac, C., Chaboureau, J.-P., Masson, V., Pinty, J.-P., Tulet, P., Escobar, J., et al. (2018). Overview of the Meso-NH model version 5.4 and its applications. *Geoscientific Model Development*, *11*, 1929–1969.

Lafore, J. P., Stein, J., Asencio, N., Bougeault, P., Ducrocq, V., Duron, J., et al. (1998). The Méso-NH atmospheric simulation system. Part I: Adiabatic formulation and control simulation. *Annales Geophysics*, *16*, 90–109.

Lancz, D., Szintai, B., & Honnert, R. (2017). Modification of shallow convection parametrization in the gray zone in a mesoscale model. *Boundary-Layer Meteorology*, *169*, 483–503.

Lappen, C.-L., & Randall, D. A. (2001). Toward a unified parameterization of the boundary layer and moist convection. Part I: A new type of mass-flux model. *Journal of the Atmospheric Sciences*, *58*(15), 2021–2036. https://doi.org/10.1175/1520-0469(2001)058<2021:TAUPOT>2.0.CO;2

Lazeroms, W. M. J., Svensson, G., Bazile, E., Brethouwer, G., Wallin, S., & Johansson, A. V. (2016). Study of transitions in the atmospheric boundary layer using explicit algebraic turbulence models. *Boundary-Layer Meteorology*, *161*(1), 19–47. https://doi.org/10.1007/s10546-016-0194-1

LeMone, M. A., Chen, F., Tewari, M., Dudhia, J., Geerts, B., Miao, Q., et al. (2010). Simulating the IHOP_2002 fair-weather CBL with the WRF-ARW-Noah modeling system. Part II: Structures from a few kilometers to 100 km across. *Monthly Weather Review*, *138*(3), 745–764. https://doi.org/10.1175/2009MWR3004.1

Lean, H. W., Clark, P. A., Dixon, M., Roberts, N. M., Fitch, A., Forbes, R., & Halliwell, C. (2008). Characteristics of high-resolution versions of the Met Office Unified Model for forecasting convection over the United Kingdom. *Monthly Weather Review*, *136*(9), 3408–3424.

Leoncini, G., Plant, R. S., Gray, S. L., & Clark, P. A. (2010). Perturbation growth at the convective scale for CSIP IOP18. *Quarterly Journal of the Royal Meteorological Society*, *136*, 653–670.

Leroyer, S., Bélair, S., Mailhot, J., & Strachan, I. B. (2011). Microscale numerical prediction over Montreal with the Canadian external urban modeling system. *Journal of Applied Meteorology and Climatology*, *50*(12), 2410–2428. https://doi.org/10.1175/JAMC-D-11-013.1

Lilly, D. K. (1967). The representation of small-scale turbulence in numerical simulation experiments. In *Proceedings of IBM Scientific Computing Symposium on Environmental Sciences* (pp. 195–210). Yorktown Heights, New York.

Lock, A. P., Brown, A. R., Bush, M. R., Martin, G. M., & Smith, R. N. B. (2000). A new boundary layer mixing scheme. Part I: Scheme description and single-column model tests. *Monthly Weather Review*, *128*(9), 3187–3199. https://doi.org/10.1175/1520-0493(2000) 128<3187:ANBLMS>2.0.CO;2

Malavelle, F. F., Haywood, J. M., Field, P. R., Hill, A. A., Abel, S. J., Lock, A. P., et al. (2014). A method to represent subgrid-scale updraft velocity in kilometer-scale models: Implication for aerosol activation. *Journal of Geophysical Research: Atmospheres*, *119*, 4149–4173. https://doi.org/10.1002/2013JD021218

Martinet, M., Nuissier, O., Duffourg, F., Ducrocq, V., & Ricard, D. (2017). Fine-scale numerical analysis of the sensitivity of the HyMeX IOP16a heavy precipitating event to the turbulent mixing-length parametrization. *Quarterly Journal of the Royal Meteorological Society*, *143*, 3122–3135. https://doi.org/10.1002/qj.3167

Mason, P. J., & Brown, A. R. (1999). On subgrid models and filter operations in large eddy simulations. *Journal of the Atmospheric Sciences*, *56*, 2101–2104.

Mason, P. J., & Thomson, D. J. (1992). Stochastic backscatter in large-eddy simulations of boundary layers. *Journal of Fluid Mechanics*, *242*, 51–78.

Mellor, G. L., & Yamada, T. (1982). Development of a turbulence closure model for geophysical fluid problems. *Reviews of Geophysics*, *20*(4), 851–875.

Mirocha, J., Kirkil, G., Bou-Zeid, E., Chow, F. K., & Kosovic, B. (2013). Transition and equilibration of neutral atmospheric boundary layer flow in one-way nested large-eddy simulations using the weather research and forecasting model. *Monthly Weather Review*, *141*, 918–940.

Muñoz-Esparza, D., Kosović, B., Mirocha, J., & van Beeck, J. (2014). Bridging the transition from mesoscale to microscale turbulence in numerical weather prediction models. *Boundary-Layer Meteorology*, *153*(3), 409–440. https://doi.org/10.1007/s10546-014-9956-9

Nakanishi, M., & Nino, H. (2009). Development of an improved turbulence closure model for the atmospheric boundary layer. *Journal of the Meteorological Society of Japan*, *87*(5), 895–912. https://doi.org/10.2151/jmsj.87.895

Neggers, R. A. J., Griewank, P. J., & Heus, T. (2019). Power-law scaling in the internal variability of cumulus cloud size distributions due to subsampling and spatial organization. *Journal of the Atmospheric Sciences*, *76*(6), 1489–1503. https://doi.org/10.1175/JAS-D-18-0194.1

Neggers, R. A. J., Koehler, M., & Beljaars, A. A. M. (2009). A dual mass flux framework for boundary-layer convection. Part I: Transport. *Journal of the Atmospheric Sciences*, *66*, 1465–1487.

Neggers, R. A. J., Siebesma, A. P., & Jonker, H. J. J. (2002). A multiparcel model for shallow cumulus convection. *Journal of the Atmospheric Sciences*, *59*, 1655–1668.

O'Neill, J. J., Cai, X.-M., & Kinnersley, R. (2015). A generalised stochastic backscatter model: Large-eddy simulation of the neutral surface layer. *Quarterly Journal of the Royal Meteorological Society*, *141*, 2617–2629.

Orlanski, I. (1975). A rational subdivison of scales for atmospheric processes. *Bulletin of the American Meteorological Society*, *56*, 527–530.

Palmer, T. N. (2001). A nonlinear dynamical perspective on model error: A proposal for non-local stochastic-dynamic parametrization in weather and climate prediction models. *Quarterly Journal of the Royal Meteorological Society*, *127*, 279–304.

Palmer, T. N. (2012). Towards the probabilistic Earth-system simulator: A vision for the future of climate and weather prediction. *Quarterly Journal of the Royal Meteorological Society*, *138*, 841–861.

Park, S. (2014). A Unified Convection Scheme (UNICON). Part I: Formulation. *Journal of the Atmospheric Sciences*, *71*, 3902–3930. https://doi.org/10.1175/JAS-D-13-0233.1

Pergaud, J., Masson, V., Malardel, S., & Couvreux, F. (2009). A parametrisation of dry thermals and shallow cumuli for mesoscale numerical weather prediction. *Boundary-Layer Meteorology*, *132*, 83–106.

Petch, J. C., Brown, A. R., & Gray, M. E. B. (2002). The impact of horizontal resolution on the simulations of convective development over land. *Quarterly Journal of the Royal Meteorological Society*, *128*, 2031–2044. https://doi.org/10.1256/003590002320603511

Plant, R. S., Bengtsson, L., & Whitall, M. A. (2015). Stochastic aspects of convective parameterization. In R. S. Plant, & J.-I. Yano (Eds.), *Parameterization of atmospheric convection. Volume 2: Current issues and new theories* (pp. 135–172). World Scientific, Imperial College Press.

Plant, R. S., & Craig, G. C. (2008). A stochastic parameterization for deep convection based on equilibrium statistics. *Journal of the Atmospheric Sciences*, *65*, 87–105.

Ramachandran, S., & Wyngaard, J. C. (2011). Subfilter-scale modelling using transport equations: Large-eddy simulation of the moderately convective atmospheric boundary layer. *Boundary-Layer Meteorology*, *139*, 1–35.

Raynaud, L., & Bouttier, F. (2017). The impact of horizontal resolution and ensemble size for convective-scale probabilistic forecasts. *Quarterly Journal of the Royal Meteorological Society*, *143*, 3037–3047.

Redelsperger, J. L., Thorncroft, C. D., A. Diedhiou, T. L., Parker, D. J., & Polcher, J. (2006). African monsoon multidisciplinary analysis an international research project and field campaign. *Bulletin of the American Meteorological Society*, *87*(12), 1735–1746.

Ricard, D., Lac, C., Legrand, R., Mary, A., & Riette, S. (2013). Kinetic energy spectra characteristics of two convection-permitting limited-area models AROME and MesoNH. *Quarterly Journal of the Royal Meteorological Society*, *139*, 1327–1341.

Rio, C., Hourdin, F., Couvreux, F., & Jam, A. (2010). Resolved versus parametrized boundary-layer plumes. Part II: Continuous formulations of mixing rates for mass-flux schemes. *Boundary-Layer Meteorology*, *135*, 469–483.

Roberts, N. M., & Lean, H. W. (2008). Scale-selective verification of rainfall accumulations from high-resolution forecasts of convective events. *Monthly Weather Review*, *136*(1), 78–97. https://doi.org/10.1175/2007MWR2123.1

Sakradzija, M., Seifert, A., & Dipankar, A. (2016). A stochastic scale-aware parameterization of shallow cumulus convection across the convective gray zone. *Journal of Advances in Modeling Earth Systems*, *8*, 786–812. https://doi.org/10.1002/2016MS000634

Sakradzija, M., Seifert, A., & Heus, T. (2014). Fluctuations in a quasi-stationary shallow cumulus cloud ensemble. *Nonlinear Processes in Geophysics*, *1*, 1223–1282.

Seity, Y., Brousseau, P., Malardelle, S., Hello, G., Bouttier, F., Lac, C., & Masson, V. (2011). The AROME-France convective scale operational model. *Monthly Weather Review*, *139*, 976–991.

Shin, H. H., & Dudhia, J. (2016). Evaluation of PBL parameterizations in WRF at subkilometer grid spacings: Turbulence statistics in the dry convective boundary layer. *Monthly Weather Review*, *144*(3), 1161–1177. https://doi.org/10.1175/MWR-D-15-0208.1

Shin, H. H., & Hong, S. (2013). Analysis on resolved and parameterized vertical transports in the convective boundary layers at the gray-zone resolution. *Journal of the Atmospheric Sciences*, *70*, 3248–3261.

Shin, H. H., & Hong, S. (2015). Representation of the subgrid-scale turbulent transport in convective boundary layers at gray-zone resolutions. *Monthly Weather Review*, *143*, 250–271.

Siebesma, A. P., & Cuijpers, J. W. M. (1995). Evaluation of parametric assumptions for shallow cumulus convection. *Journal of the Atmospheric Sciences*, *52*(6), 650–666.

Siebesma, P., Jakob, C., Lenderink, G., Neggers, R. A. J., Teixeira, J., van Meijgaard, E., et al. (2004). Cloud representation in general-circulation models over the northern Pacific ocean: A EUROCS intercomparison study. *Quarterly Journal of the Royal Meteorological Society*, *130*, 3245–3267.

Siebesma, A. P., Soares, P. M. M., & Teixeira, J. (2007). A combined eddy-diffusivity mass-flux approach for the convective boundary layer. *Journal of the Atmospheric Sciences*, *64*, 1230–1248.

Simon, J. S., Zhou, B., Mirocha, J. D., & Chow, F. K. (2019). Explicit filtering and reconstruction to reduce grid dependence in convective boundary layer simulations using WRF-LES. *Monthly Weather Review*, *147*, 1805–1821. https://doi.org/10.1175/MWR-D-18-0205.1

Skamarock, W. C. (2004). Evaluating mesoscale NWP models using kinetic energy spectra. *Monthly Weather Review*, *132*, 3019–3032.

Smagorinsky, J. J. (1967). General circulation experiments with the primitive equations. *Monthly Weather Review*, *91*(3), 99–164. https://doi.org/10.1175/1520-0493(1963)091<0099:GCEWTP>2.3.CO;2

Stein, T. H. M., Hogan, R. J., Clark, P. A., Halliwell, C. E., Hanley, K. E., Lean, H. W., et al. (2015). The DYMECS project: A statistical approach for the evaluation of convective storms in high-resolution NWP models. *Bulletin of the American Meteorological Society*, *96*, 939–951.

Stirling, A. J., & Petch, J. C. (2004). The impacts of spatial variability on the development of convection. *Quarterly Journal of the Royal Meteorological Society*, *130*, 3189–3206.

Stoelinga, M. T. (1996). A potential vorticity-based study on the role of diabatic heating and friction in a numerically simulated baroclinic cyclone. *Monthly Weather Review*, *124*, 849–874.

Stull, R. B. (1984). Transilient turbulence theory. Part I: The concept of eddy-mixing across finite distances. *Journal of the Atmospheric Sciences*, *41*, 3351–3366.

Stull, R. B. (1988). *An introduction to boundary layer meteorology* (pp. 666). Dordrecht, Boston and London: Kluwer Academic Publishers. https://doi.org/10.1007/978-94-009-3027-8

Sullivan, P. P., Horst, T. W., Lenschow, D. H., Moeng, C.-H., & Weil, J. C. (2003). Structure of subfilter-scale fluxes in the atmospheric surface layer with application to large-eddy simulation modelling. *Journal of Fluid Mechanics*, *482*, 101–139.

Sullivan, P. P., McWilliams, J. C., & Moeng, C.-H. (1996). A grid nesting method for large-eddy simulation of planetary boundary-layer flows. *Boundary-Layer Meteorology*, *80*(1-2), 167–202.

Sullivan, P. P., & Patton, E. G. (2011). The effect of mesh resolution on convective boundary layer statistics and structures generated by large-eddy simulation. *Journal of the Atmospheric Sciences*, *68*(10), 2395–2415. https://doi.org/10.1175/JAS-D-10-05010.1

Suselj, K., Hogan, T. F., & Teixeira, J. (2014). Implementation of a stochastic eddy-diffusivity/mass-flux parameterization into the Navy Global Environmental Model. *Weath and Forecasting*, *29*, 1374–1390. https://doi.org/10.1175/WAF-D-14-00043.1

Tan, Z., Kaul, C. M., Pressel, K. G., Cohen, Y., Schneider, T., & Teixeira, J. (2018). An extended eddy-diffusivity mass-flux scheme for unified representation of subgrid-scale turbulence and convection. *Journal of Advances in Modeling Earth Systems*, *10*, 770–800. https://doi.org/10.1002/2017MS001162

Teixeira, J., & Cheinet, S. (2004). A simple mixing length formulation for the eddy-diffusivity parameterization of dry convection. *Boundary-Layer Meteorology*, *110*(3), 435–453.

Thuburn, J., Weller, H., Vallis, G. K., Beare, R. J., & Whitall, M. (2018). A framework for convection and boundary layer parameterization derived from conditional filtering. *Journal of the Atmospheric Sciences*, *75*(3), 965–981. https://doi.org/10.1175/JAS-D-17-0130.1

Tomassini, L., Field, P. R., Honnert, R., Malardel, S., McTaggart-Cowan, R., Saitou, K., et al. (2016). The grey zone cold air outbreak global model intercomparison: A cross evaluation using large-eddy simulations. *Journal of Advances in Modeling Earth Systems*, *9*, 39–64. https://doi.org/10.1002/2016MS000822

Tomassini, L., Parker, D. J., Stirling, A., Bain, C., Senior, C., & Milton, S. (2017). The interaction between moist diabatic processes and the atmospheric circulation in African Easterly Wave propagation. *Quarterly Journal of the Royal Meteorological Society*, *143*, 3207–3227.

Verrelle, A., Ricard, D., & Lac, C. (2015). Sensitivity of high-resolution idealized simulations of thunderstorms to horizontal resolution and turbulence parametrization. *Quarterly Journal of the Royal Meteorological Society*, *141*, 433–448.

Verrelle, A., Ricard, D., & Lac, C. (2017). Evaluation and improvement of turbulence parameterization inside deep convective clouds at kilometer-scale resolution. *Monthly Weather Review*, *145*(10), 3947–3967. https://doi.org/10.1175/MWR-D-16-0404.1

Wagner, J. S., Gohm, A., & Rotach, M. W. (2014). The impact of horizontal model grid resolution on the boundary layer structure over an idealized valley. *Monthly Weather Review*, *142*(9), 3446–3465.

Wagner, T. M., & Graf, H.-F. (2010). An ensemble cumulus convection parameterization with explicit cloud treatment. *Journal of the Atmospheric Sciences*, *67*, 3854–3869.

Warren, R. A., Kirshbaum, D. J., Plant, R. S., & Lean, H. W. (2014). A Boscastle-type quasi-stationary convective system over the UK southwest peninsula. *Quarterly Journal of the Royal Meteorological Society*, *140*(678), 240–257.

Weckwerth, T. M., Parsons, D. B., Koch, S. E., Moore, J. A., LeMone, M. A., Demoz, B. B., et al. (2004). An overview of the International H2O Project (IHOP_2002) and some preliminary highlights. *Bulletin of the American Meteorological Society*, *85*(2), 253–278. https://doi.org/10.1175/BAMS-85-2-253

Weinbrecht, S., & Mason, P. J. (2008). Stochastic backscatter for cloud-resolving models. Part I: Implementation and testing in a dry convective boundary layer. *Journal of the Atmospheric Sciences*, *65*, 123–139.

Wyngaard, J. C. (2004). Toward numerical modelling in the "Terra Incognita". *Journal of the Atmospheric Sciences*, *61*, 1816–1826.

Xie, Z.-T., & Castro, I. P. (2008). Efficient generation of inflow conditions for large eddy simulation of street-scale flows. *Flow, Turbulence and Combustion*, *81*, 449–470.

Young, G. S., Kristovich, D. A. R., Hjelmfelt, M. R., & Foster, R. C. (2002). Rolls, streets, waves, and more: A review of quasi-two-dimensional structures in the atmospheric boundary layer. *Bulletin of the American Meteorological Society*, *83*(7), 997–1002.

Zhang, X., Bao, J.-W., Chen, B., & Grell, E. D. (2018). A three-dimensional scale-adaptive turbulent kinetic energy scheme in the WRF-ARW model. *Monthly Weather Review*, *146*(7), 2023–2045. https://doi.org/10.1175/MWR-D-17-0356.1

Zhou, B., Simon, J. S., & Chow, F. K. (2014). The convective boundary layer in the terra incognita. *Journal of the Atmospheric Sciences*, *71*(7), 2545–2563. https://doi.org/10.1175/JAS-D-13-0356.1

Zhou, B., Xue, M., & Zhu, K. (2017). A grid-refinement-based approach for modeling the convective boundary layer in the gray zone: A pilot study. *Journal of the Atmospheric Sciences*, *74*(11), 3497–3513. https://doi.org/10.1175/JAS-D-16-0376.1

Zhou, B., Xue, M., & Zhu, K. (2018). A grid-refinement-based approach for modeling the convective boundary layer in the gray zone: Algorithm implementation and testing. *Journal of the Atmospheric Sciences*, *75*(4), 1143–1161. https://doi.org/10.1175/JAS-D-17-0346.1

Erratum

In the originally published version of this article, an in-text citation to Ramachandran et al. (2013) was erroneously included in section 3.1, and the corresponding reference appeared in the References: Ramachandran, S., Tandon, A., & Mahadevan, A. (2013). Effect of subgrid-scale mixing on the evolution of forced submesoscale instabilities. Ocean Modelling, 66, 45–63. The article has since been corrected, and this version may be considered the authoritative version of record.